Decay of the de Sitter vacuum

Paul R. Anderson, Emil Mottola, and Dillon H. Sanders

Phys. Rev. D **97**, 065016 — Published 27 March 2018

DOI: 10.1103/PhysRevD.97.065016

LA-UR-17-28548

Decay of the de Sitter Vacuum

Paul R. Anderson[a],* Emil Mottola[b],† and Dillon H. Sanders[a]

[a)] *Department of Physics,*
Wake Forest University,
Winston-Salem, NC 27109, USA
and
[b)] *Theoretical Division, T-2, MS B285*
Los Alamos National Laboratory
Los Alamos, NM 87545 USA

The decay rate of the Bunch-Davies state of a massive scalar field in the expanding flat spatial sections of de Sitter space is determined by an analysis of the particle pair creation process in real time. The Feynman definition of particle and antiparticle Fourier mode solutions of the scalar wave equation, and their adiabatic phase analytically continued to the complexified time domain, show conclusively that the Bunch-Davies state is not the vacuum state at late times. The closely analogous creation of charged particle pairs in a uniform electric field is reviewed and Schwinger's result for the vacuum decay rate is recovered by this same real time analysis. The vacuum decay rate in each case is also calculated by switching the background field on adiabatically, allowing it to act for a very long time, and then adiabatically switching it off again. In both the uniform electric field and de Sitter cases the particles created while the field is switched on are verified to be real, in the sense that they persist in the final asymptotic flat zero-field region. In the de Sitter case there is an interesting residual dependence of the rate on how the de Sitter phase is ended, indicating a greater sensitivity to spatial boundary conditions. The electric current of the created particles in the E-field case and their energy density and pressure in the de Sitter case are also computed, and the magnitude of their backreaction effects on the background field estimated. Possible consequences of the Hubble scale instability of the de Sitter vacuum for cosmology, vacuum dark energy, and the cosmological 'constant' problem are discussed.

* anderson@wfu.edu
† emil@lanl.gov

I. INTRODUCTION

The vacuum state of quantum field theory (QFT) in flat Minkowski space, with no external fields, is defined as the eigenstate of the Hamiltonian with the lowest eigenvalue. The existence of a Hamiltonian generator of time translational symmetry, with a non-negative spectrum, bounded from below is crucial to the existence and determination of the vacuum ground state, containing no particle excitations. Particle states are defined then by solutions of relativistic wave equations forming irreducible representations of the Poincaré group. The vacuum state is invariant under translations, rotations and Lorentz boosts, and the correlation functions built upon this vacuum state enjoy complete invariance under Poincaré symmetry.

As is well known, these properties do not hold in a general curved spacetime, in time dependent external background fields, nor even for a free QFT in flat spacetime under general coordinate transformations that are not Poincaré symmetries. In these cases the Hamiltonian becomes time dependent or no Hamiltonian bounded from below exists at all, and the concepts of 'vacuum' or 'particles' become much more subtle. In situations when the background has a high degree of symmetry, such as de Sitter spacetime, it has been customary to avoid the particle concept altogether, and focus attention instead on the state possessing the maximal symmetry of the background. In de Sitter space this maximal $O(4,1)$ symmetric state for massive fields is commonly known as the Bunch-Davies state.[1] The question of whether the Bunch-Davies state is actually a 'vacuum' state, or a stable state at all has been the subject of a number of investigations [3–6], although with implications that appear to differ somewhat from each other, even for free fields [7, 8]. When self-interactions are considered, additional differences between the various approaches arise [9–19]. At yet another level are the potential effects of graviton loops, when higher order gravitational interactions are considered [20].

In view of the central role the Bunch-Davies state plays in cosmological models of inflation and the origin of fluctuations that give rise to anisotropies in the universe [21], as well as the importance of de Sitter vacuum instability to the fundamental issue of vacuum energy in cosmology and the cosmological constant problem [22–24], it is essential that the physical basis of the QFT vacuum in de Sitter space be clearly established. Reconciling the various approaches to vacuum energy in cosmology when the technical issues that arise in the cases interactions, light fields, or graviton loops are considered, is bound to be more difficult if de Sitter vacuum decay in the simplest and best controlled case of a massive scalar free field is not first fully clarified.

[1] The state was first investigated by several authors [1, 2] and might also be called the Chernikov-Tagirov-Bunch-Davies (CTBD) state.

To this end in this paper we discuss in detail the close correspondence between QFT in de Sitter spacetime and in the non-gravitational background of a constant, uniform electric field [5], which provides important guidance for the de Sitter case. Both backgrounds have a high degree of symmetry, which permit exact solutions and natural generalizations of concepts and QFT methods from the case of a flat, zero-field background. Yet neither admit a conserved Hamiltonian bounded from below, and in both cases particle creation occurs and vacuum decay is expected.

In the case of a constant, uniform electric field, the QFT of charged matter, neglecting self-interactions, was considered by Schwinger in the covariant proper time representation [25]. By this covariant heat kernel method the vacuum decay probability and decay rate in terms of the imaginary part of the one-loop effective action is obtained, defined by analytic continuation in the proper time variable. Since the E-field spontaneously decays into particle/antiparticle pairs, the 'vacuum' is *not* the state of maximal symmetry of the background (which is time reversal symmetric), but instead the E-field initiates a non-trivial time dependent process, which almost certainly leads to a state populated with particle/antiparticle excitations in which the coherent mean electric field vanishes asymptotically at late times. The correspondence with the de Sitter case suggests that cosmological vacuum energy should similarly decay into particle/antiparticle pairs, eventually leading to a state with small but non-zero slowly decaying vacuum energy [3, 24].

Schwinger's proper time method makes no explicit reference to particles, and its very elegance disguises somewhat the physical definition of vacuum it entails. Later studies of QFT in a constant E-field by canonical quantization methods [26–30] revealed that the essential ingredient is the $m^2 \to m^2 - i\epsilon$ prescription where $\epsilon \to 0^+$. This is of course the same $i\epsilon$ prescription defining the causal propagator function in flat space QFT, which Feynman obtained by identifying positive frequency solutions of the wave equation as particles propagating forward in time, and negative frequency solutions as the corresponding antiparticles propagating backward in time [31]. It is this physical condition that provides the mathematically precise definition of particle/antiparticle excitations and fixes the vacuum state of relativistic QFT in *real* time, which by continuity and the adiabatic theorem applies also to background fields or weakly curved spacetimes.

The $m^2 - i\epsilon$ rule in the Schwinger proper time approach is specified by a single exponential describing a relativistic particle worldline. Causality is enforced by the particle always moving forward in its own proper time, whether the external coordinate time t does so or not. This observation, first made by Stueckelberg [32], carries over unaltered to curved spacetimes. The extension of the covariant Schwinger heat kernel method to gravitational backgrounds was developed extensively by DeWitt [33]. The causality condition and m^2 analyticity it implies in the covariant

Schwinger-DeWitt formulation is mathematically equivalent to the requirement that ingoing particle modes as $t \to -\infty$ are analytic in the *upper* half complex m^2 plane, while the corresponding outgoing modes as $t \to +\infty$ are analytic in the *lower* half complex m^2 plane [34, 35]. Antiparticle modes are the complex conjugate solutions of the wave equation in which the analyticity requirements in the upper/lower m^2 plane are reversed. It is not difficult to see that the definition of the corresponding $|0, in\rangle$ and $|0, out\rangle$ vacuum states, and the *in-out* effective action they imply, leads to a non-trivial Bogoliubov transformation between the $|0, in\rangle$ and $|0, out\rangle$ states, particle pair creation and a vacuum decay rate for de Sitter space analogous to that of the uniform E-field [3, 5].

In the canonical description in terms of Fock space creation and destruction operators, pair creation manifests as a non-trivial Bogoliubov transformation between the positive/negative frequency operators as $t \to -\infty$, which define the $|0, in\rangle$ vacuum, relative to the corresponding positive/negative frequency operators as $t \to +\infty$ which define the $|0, out\rangle$ vacuum. The overlap probability

$$\left|\langle 0, out|0, in\rangle\right|^2_{V,T} = \exp\left\{-VT\,\Gamma\right\} = \exp\left\{-2\,VT\,\mathrm{Im}\,\mathcal{L}_{\rm eff}\right\} \tag{1.1}$$

behaves exponentially in the spatial volume V and time T that the background field is applied, with $\Gamma = 2\,\mathrm{Im}\,\mathcal{L}_{\rm eff}$ twice the imaginary part of the effective Lagrangian density $\mathcal{L}_{\rm eff}$ found by the Schwinger proper time approach. To be meaningful the four-volume factor $\mathcal{V}_4 = VT$ must be removed from (1.1). For persistent symmetric backgrounds $\mathcal{L}_{\rm eff}$ is independent of the spacetime coordinates $\mathbf{x}$ and t. Then Γ is the constant decay rate of the $|0, in\rangle$ vacuum per unit volume per unit time due to steady spontaneous creation of particle/antiparticle pairs by the fixed classical (E or de Sitter) background field, under the assumption that the space and time dependence of the background and any backreaction may be neglected at lowest order. Notice that the effective action and the vacuum decay rate given by its imaginary part in (1.1) are coordinate invariant quantities, even though the space+time splitting, and definition of positive/negative frequency modes, Bogoliubov transformation, and definition of particles is not. General coordinate invariance is manifest throughout only in the Schwinger-DeWitt worldline proper time representation.

It is important also to realize that the imaginary part of the one-loop effective Lagrangian $\mathrm{Im}\,\mathcal{L}_{\rm eff}$, and vacuum decay rate Γ cannot be obtained by reliance upon a calculation in Euclidean time $\tau = it$, but instead requires a definition of the vacuum consistent with causality in *real* time. Indeed, since the electric field is the F_{j0} component of the field strength tensor, a Euclidean calculation with $E_j = F_{j0} \to iF_{j4}$ in this case would be tantamount to treating it as a constant *magnetic* field background $B_i = \frac{1}{2}\epsilon_{ijk}F_{jk}$, for which the quantum Hamiltonian is bounded from below, par-

ticle trajectories are circular rather than hyperbolic, no particle creation at all occurs, and the vacuum is stable, all of which is completely different physics than the E-field background in real time. Including particle self-interactions does not change these fundamental differences between backgrounds for which the Lorentz invariant quantity $\mathbf{B}^2 - \mathbf{E}^2$ has opposite signs. An interacting QFT built upon the B-field vacuum with Euclidean time correlation functions is therefore necessarily *physically inequivalent* to the E-field in real time, completely missing the particle pair creation and vacuum decay rate contained in (1.1), *even at lowest zeroth order* in the self-interactions.

At the particle worldline level the vacuum decay is typified by hyperbolic trajectories of constant acceleration of particles in an electric field, in contrast to the closed circular orbits in the corresponding Euclidean constant magnetic field, which does possess a stable QFT vacuum. The hyperbolic trajectories of freely falling test particles in de Sitter space, drawn away from each other by the de Sitter expansion are similarly clearly different qualitatively from the closed circular trajectories of test particles on the compact Euclidean $\mathbb{S}^4$ manifold. Since analytic continuation of propagators to the Euclidean $\mathbb{S}^4$ manifold enforces boundary conditions whose semi-classical limit are precisely these closed circular trajectories, it defines a theory inequivalent to that on the Lorentzian de Sitter manifold which requires quite different boundary conditions at asymptotic early and late times $t \to \mp\infty$, even in the absence of self-interactions. These different boundary conditions lead to the instability of the Bunch-Davies state to particle creation in real time.

This essential difference between specification of the vacuum in real time and the postulate of Euclidean analyticity is one of the root causes of the different results and claims in the literature. The difference between the $m^2 - i\epsilon$ prescription *vs.* Euclidean continuation is not simply a difference of formalisms, but rather of enforcing completely different physical requirements on the QFT vacuum by different initial/final conditions in real time than those imposed by regularity in the Euclidean time domain. Although equivalent in flat Minkowski space, it turns out that the $m^2 - i\epsilon$ prescription required by causality is *mathematically inconsistent* with Euclidean continuation in background fields such as the E-field or de Sitter space, and leads to physically different results.

One way of seeing why the equivalence of Euclidean continuation to the causal QFT vacuum in flat space fails to hold in de Sitter space is in the qualitatively different properties of representations of the Poincaré and de Sitter symmetry groups. It is an important special property of Minkowski spacetime that the subspaces of positive and negative frequency solutions of the wave equation are *separately* invariant under proper orthochronous Lorentz transformations, so that the Stueckelberg-Feynman definition of vacuum is consistent with maximal Poincaré symmetry. In contrast, there is *no* $SO(4,1)$ invariant decomposition of positive and negative frequency solutions in de Sitter

spacetime. Any such decomposition into positive and negative frequency subspaces *mix* under $SO(4,1)$ symmetry transformations, and transform with equivalent representations of the de Sitter group [36]. As a result there is no de Sitter invariant way to distinguish particles from antiparticles, and no reason for the physical Stueckelberg-Feynman definition of particle excitations or vacuum to lead to a de Sitter invariant state. Indeed on any finite time slice, it does not.

Closely related to and following from analyticity requirements in m^2, rather than a Euclidean postulate, is the fact that the de Sitter/Feynman propagator $G_F(x,x')$ calculated with *in-out* boundary conditions obeys the composition rule

$$\int_{\Sigma_x} d\Sigma_x^\mu \; G_F(x_1,x) \overset{\leftrightarrow}{\nabla}_\mu G_F(x,x_2) = G_F(x_1,x_2) \tag{1.2}$$

consistent with causality, where Σ_x is an arbitrary spacelike surface intermediate between x_1 and x_2. This composition rule again expresses the Stueckelberg-Feynman prescription of particles moving forward in time, antiparticles backward in time, and results from the representation of G_F in terms of a single exponential in worldline proper time in Schwinger's method, rather than a sum of exponentials of opposite sign. These single exponentials combine simply and lead to the composition (1.2), which is *violated* by the Euclidean Bunch-Davies propagator [4]. In physical terms the Bunch-Davies state is best understood not as a 'vacuum' state at all, but as a particular finely tuned phase coherent superposition of particle and antiparticle modes [5].

In this paper we study the process of particle creation in greater detail in real time, using the flat Poincaré spatial slicing of de Sitter space most commonly considered in cosmology. The m^2 analyticity properties of the complex Fourier mode function solutions of the scalar wave equation (2.2) defining particle and antiparticle waves according to the Feynman description lead directly to consideration of the adiabatic phase integral (2.9), and the concept of adiabatic particle creation [37–40]. The analytic extension of the adiabatic phase to the complex time domain allows for determination of the time $t_{\rm event}(\mathbf{k})$ at which each Fourier mode labeled by $\mathbf{k}$ most probably experiences a particle creation event. Determination of $t_{\rm event}(\mathbf{k})$ relates the interval of time during which the external (E-field or de Sitter) field is applied to the range of Fourier modes contributing to the decay rate (2.23), allowing for the infinite four-volume factor $\mathcal{V}_4$ to be removed, thereby determining the finite rate Γ and pre-factor in (2.24) unambiguously for persistent background fields.

We also consider the vacuum decay rate Γ obtained by adiabatically turning the electric or expanding de Sitter background field on and then off again, after the lapse of a long but finite time T. In this approach there can be no ambiguity of initial and final vacuum states, since the geometry

at both early ($t \to -\infty$) and late ($t \to +\infty$) times is Minkowski flat space with zero background field. Both approaches remove the somewhat unsatisfactory feature of previous constant E-field or de Sitter background calculations, in which a formal divergence in the integral over modes must be cut off by appeal to the finite 'window' of modes undergoing particle creation in a finite time T in the constant background [5, 26–28]. When the two approaches are applicable they would be expected to yield the same result, and they do for the E-field background. However, in the de Sitter case the second method reveals a possibly unexpected sensitivity to the details of how the de Sitter expansion is ended, which suggests sensitivity to infrared spatial boundary conditions and correlations over superhorizon scales that may have important implications for cosmology.

The outline of the paper is as follows. The next section reviews the general framework of particle creation and vacuum decay by means of the adiabatic phase and non-uniformity of the adiabatic condition in persistent background fields. Sec. III shows how the adiabatic phase integral, and its Stokes lines of constant Real Part in the complex plane can be used to determine the time $t_{\rm event}$ of a particle creation event, which applied to the case of a constant, uniform electric field reproduces Schwinger's result for the vacuum decay of the E-field. In Sec. IV two time profiles of the uniform electric field for which it is adiabatically turned on and off with a long duration T in between where it is constant are used to compute the particle creation and decay rate in the limit $T \to \infty$, again reproducing the Schwinger result. The electric current is also computed for one profile and shown to grow linearly with T, so that the secular effects of backreaction clearly must be taken into account for persistent fields. In Sec. V, the same adiabatic phase method is applied to a persistent de Sitter background in the spatially flat Poincaré coordinates, and the particle creation and finite decay rate of the Bunch-Davies state determined. In Sec. VI we consider two time profiles for which the de Sitter background is adiabatically turned on and off with a long time duration in between, similar to the E-field case. For one profile we evaluate the particle creation and decay rate numerically in the limit of long time duration. In Sec. VII an analytic estimate is made of the energy density and pressure of the particles created in the de Sitter phase along with an estimate of the strength of their backreaction effect. Sec. VIII contains a discussion of our conclusions including the possible implications for inflation, vacuum dark energy, and the cosmological 'constant' problem.

II. PARTICLE CREATION AND THE ADIABATIC PHASE

We consider a quantum field interacting only with a classically prescribed (*i.e.* non-dynamical) external background field. For simplicity we specialize to a non-self-interacting scalar field Φ and a spatially homogeneous but time-dependent classical background. Making use of spatial homogeneity, the quantum scalar field operator in flat space may be expanded in a Fourier series

$$\Phi(t,\mathbf{x}) = \frac{1}{\sqrt{V}} \sum_{\mathbf{k}} \Big\{ a_{\mathbf{k}}\, e^{i\mathbf{k}\cdot\mathbf{x}}\, f_{\mathbf{k}}(t) + b^{\dagger}_{\mathbf{k}}\, e^{-i\mathbf{k}\cdot\mathbf{x}}\, f^{*}_{\mathbf{k}}(t) \Big\} \tag{2.1}$$

whose time-dependent mode functions obey second order differential equations in time of the form

$$\left[\frac{d^2}{dt^2} + \omega^2_{\mathbf{k}}(t) \right] f_{\mathbf{k}}(t) = 0 \, . \tag{2.2}$$

Here $\mathbf{k}$ labels the spatial momentum which takes on discrete values for periodic boundary conditions in the finite volume V. For the cases of interest in this paper $\omega^2_{\mathbf{k}}(t)$ is a real time-dependent frequency function that for massive fields is strictly positive, nowhere vanishing on the real time axis $-\infty < t < \infty$.

Considering the case of a charged complex scalar field $\Phi(t,\mathbf{x})$ in a pure electric field background $\mathbf{E}$, the Klein-Gordon wave equation $(\partial_\mu - ieA_\mu)^2\Phi = m^2\Phi$ gives

$$\omega^2_{\mathbf{k}}(t) = \big(\mathbf{k} - e\mathbf{A}(t)\big)^2 + m^2 \tag{2.3}$$

in the $A_0 = 0$ gauge in which $\mathbf{E} = -\dot{\mathbf{A}}$. The case of an uncharged Hermitian scalar field (obeying $\Phi^\dagger = \Phi$ and $a_{\mathbf{k}} = b_{\mathbf{k}}$) in a spatially homogeneous and isotropic cosmological spacetime may also be reduced to a mode equation of the form (2.2) with a different $\omega^2_{\mathbf{k}}(t)$: *cf.* (5.2).

The complex valued solutions of (2.2) are required to satisfy the Wronskian condition

$$f_{\mathbf{k}}\dot{f}^{*}_{\mathbf{k}} - \dot{f}_{\mathbf{k}} f^{*}_{\mathbf{k}} = i\hbar \tag{2.4}$$

constant in time, and the Fock space operators are required to obey the commutation relations

$$[a_{\mathbf{k}}, a^{\dagger}{}_{\mathbf{k}'}] = [b_{\mathbf{k}}, b^{\dagger}{}_{\mathbf{k}'}] = \delta_{\mathbf{k},\mathbf{k}'} \tag{2.5}$$

in order for the Heisenberg field operator Φ to satisfy the canonical equal time commutation relation

$$\left[\Phi(t,\mathbf{x}), \frac{\partial \Phi^\dagger}{\partial t}(t,\mathbf{x}') \right] = i\hbar\, \delta^3(\mathbf{x}-\mathbf{x}') \tag{2.6}$$

in a finite volume V. In the absence of any external field, $\mathbf{A}$ and $\omega_{\mathbf{k}}$ are constants, and

$$f^{(0)}_{\mathbf{k}}(t) \equiv \sqrt{\frac{\hbar}{2\omega_{\mathbf{k}}}}\, e^{-i\omega_{\mathbf{k}} t} \tag{2.7}$$

defines the *positive* energy particle mode function that is analytic in the *upper* half complex m^2 plane in *both* limits $t \to \mp\infty$. The corresponding Minkowski no-particle state $|0\rangle$ defined by

$$a_{\mathbf{k}}\,|0\rangle = b_{\mathbf{k}}\,|0\rangle = 0\,, \qquad \forall \quad \mathbf{k} \tag{2.8}$$

is both the vacuum $|0, in\rangle$ state and the vacuum $|0, out\rangle$ state for all times, and there is no spontaneous particle creation or vacuum instability in flat Minkowski spacetime.

The physical basis for extending the definition of no-particle vacuum states to the case of slowly varying weak external fields is the adiabatic theorem, which guarantees that the state of a quantum system does not change if subjected to an external perturbation that is arbitrarily slowly varying in time [41]. Hence in weak or slowly varying external fields the QFT vacuum must be 'close' to that of (2.7)-(2.8) and well-determined up to small terms in an asymptotic expansion of the solution of (2.2) in terms of the time derivatives of $\omega_{\mathbf{k}}$. The adiabatic phase integral

$$\Theta_{\mathbf{k}}(t) = \int^t dt'\,\omega_{\mathbf{k}}(t') \tag{2.9}$$

then takes on fundamental importance, since the zeroth order adiabatic mode function

$$\tilde{f}^{(0)}_{\mathbf{k}}(t) \equiv \frac{1}{\sqrt{2\omega_{\mathbf{k}}(t)}}\,\exp\left\{-\,i\,\Theta_{\mathbf{k}}(t)\right\} \tag{2.10}$$

is an approximate positive frequency (particle) solution to (2.2) satisfying (2.4) (with $\hbar = 1$ hereafter) in the limit that $\omega^2_{\mathbf{k}}(t)$ is an arbitrarily slowly varying function of t. Higher order approximate adiabatic mode functions $\tilde{f}^{(n)}_{\mathbf{k}}$ may be found by substituting the exponential ansatz

$$f_{\mathbf{k}}(t) = \frac{1}{\sqrt{2W_{\mathbf{k}}(t)}}\,\exp\left\{-i\int^t dt' W_{\mathbf{k}}(t')\right\} \tag{2.11}$$

into the mode eq. (2.2), resulting in the *exact* nonlinear equation for $W_{\mathbf{k}}(t)$

$$W^2_{\mathbf{k}} = \omega^2_{\mathbf{k}} + \frac{3}{4}\frac{\dot{W}^2_{\mathbf{k}}}{W^2_{\mathbf{k}}} - \frac{1}{2}\frac{\ddot{W}_{\mathbf{k}}}{W_{\mathbf{k}}} \tag{2.12}$$

which then may be expanded in an asymptotic series in time derivatives:

$$W_{\mathbf{k}} = \omega_{\mathbf{k}}\left\{1 + \frac{3}{8}\frac{\dot{\omega}^2_{\mathbf{k}}}{\omega^4_{\mathbf{k}}} - \frac{1}{4}\frac{\ddot{\omega}_{\mathbf{k}}}{\omega^3_{\mathbf{k}}} + \ldots\right\}\,. \tag{2.13}$$

Clearly the lowest (zeroth) order adiabatic mode function (2.10) with $W^{(0)}_{\mathbf{k}}(t) = \omega_{\mathbf{k}}(t)$ is a good approximation to the solution of (2.2), and the adiabatic theorem is applicable only to the extent that the relative size of the corrections in (2.13) parametrized by

$$|\delta_{\mathbf{k}}(t)| \equiv \left|\frac{3}{8}\frac{\dot{\omega}^2_{\mathbf{k}}}{\omega^4_{\mathbf{k}}} - \frac{1}{4}\frac{\ddot{\omega}_{\mathbf{k}}}{\omega^3_{\mathbf{k}}}\right| \ll 1 \tag{2.14}$$

remain uniformly small for all t.

For $\mathbf{k}$ such that (2.14) holds, $\tilde{f}^{(0)}_{\mathbf{k}}(t)$ remains an approximate positive frequency particle solution with the required analyticity in m^2 for all time, and particle creation in these Fourier modes is negligibly small. Since $|\delta_{\mathbf{k}}| \to 0$ as $|\mathbf{k}| \to \infty$, the adiabatic condition (2.14) does hold arbitrarily accurately in this limit for smoothly varying background fields with bounded time derivatives. Thus there is no particle creation in arbitrarily high momentum modes, and the vacuum remains the vacuum at large momenta or short distances. It is just this property that makes the adiabatic expansion useful for renormalization of composite operators such as the electric current or energy-momentum tensor in smoothly time varying backgrounds, requiring only the standard counterterms expected on the basis of usual power counting arguments [40, 42].

If on the other hand the condition (2.14) fails to hold at some times, and particularly at small to moderate $|\mathbf{k}|$, on the scale of the time variation of the background field, these Fourier modes will then receive some admixture of the complex conjugate approximate solution to (2.10). Because of the association of the complex conjugate solution to negative energy or antiparticle modes in (2.1) by the $m^2 - i\epsilon$ prescription, the violation of the adiabatic approximation near the maxima of $|\delta_{\mathbf{k}}(t)|$ corresponds to particle/antiparticle pairs being created spontaneously from the vacuum [37–39].

The adiabatic mode functions (2.10), perhaps extended by use of a frequency function of higher order in the asymptotic expansion (2.13), also provide useful templates against which the exact mode function solutions of (2.2) may be compared. The transformation between the two bases of $f_{\mathbf{k}}$ and $\tilde{f}^{(n)}_{\mathbf{k}}$ defines a time-dependent Bogoliubov transformation which may be used to define a semi-classical time-dependent particle number [5, 43–45]

$$\mathcal{N}^{(n)}_{\mathbf{k}}(t) = \frac{1}{2W^{(n)}_{\mathbf{k}}} \left| \dot{f}_{\mathbf{k}} + \left(iW^{(n)}_{\mathbf{k}} - \frac{V^{(n)}_{\mathbf{k}}}{2} \right) f_{\mathbf{k}} \right|^2 \tag{2.15}$$

with respect to the n^{th} order adiabatic basis functions defined by the pair of real time-dependent functions $\{W^{(n)}_{\mathbf{k}}(t), V^{(n)}_{\mathbf{k}}(t)\}$ chosen to match the asymptotic expansion (2.13) for $W_{\mathbf{k}}$ and $-\dot{W}_{\mathbf{k}}/W_{\mathbf{k}}$ respectively to n^{th} order in time derivatives. This definition is *local in time*, and has some necessary arbitrariness in that a choice of adiabatic order n must be made. Generally the lowest order $n = 0, 1, 2, \ldots$ approximations are the most useful for applications, such as defining an approximate particle number density for transition to a semi-classical Boltzmann-Vlasov transport description of non-equilibrium relativistic quantum systems [43], and in particular allowing dissipative particle interactions to be taken into account.

In this paper we focus on the application of the adiabatic method to background fields that are

persistent for long periods of time, such as constant uniform electric fields, or de Sitter space. In both cases the adiabatic condition (2.14) holds arbitrarily accurately *asymptotically* as $t \to \mp\infty$, for *any finite* $\mathbf{k}$, and asymptotic $|0, in\rangle$ and $|0, out\rangle$ vacuum states can be defined, accompanied by well-defined particle number Fock basis operators. However, since the condition (2.14) is not satisfied at all intermediate times for some $\mathbf{k}$, the approximate solution (2.10) is not a solution to the exact eq. (2.2) uniformly valid for all t, $|0, out\rangle \neq |0, in\rangle$, and particle creation occurs in such non-trivial persistent background fields. This specification of vacuum states in the asymptotic past or future is necessarily a *global in time* definition, that describes *secular* or long time effects.

In this case the task is to determine the admixture of the negative frequency complex conjugate solution at late times, $t \to +\infty$, given that the exact solution $f_{\mathbf{k}}(t)$ is a pure positive frequency solution of the form (2.10) at early times, $t \to -\infty$, or in other words, to determine the *time-independent* Bogoliubov coefficients $(A_{\mathbf{k}}, B_{\mathbf{k}})$ for the *exact* solutions of (2.2) satisfying the asymptotic conditions

$$f_{\mathbf{k}}(t) \to \begin{cases} \tilde{f}^{(0)}_{\mathbf{k}}(t)\,, & t \to -\infty \\ A_{\mathbf{k}}\, \tilde{f}^{(0)}_{\mathbf{k}}(t) + B_{\mathbf{k}}\, \tilde{f}^{(0)*}_{\mathbf{k}}(t)\,, & t \to +\infty \end{cases} \tag{2.16}$$

which has the form of a one-dimensional scattering problem. It is *'over-the-barrier'* scattering if $\omega^2_{\mathbf{k}}(t)$ is strictly positive for all real t, so that there are no classical turning points on the real t axis.

Because of the Wronskian condition (2.4), the Bogoliubov coefficients necessarily satisfy

$$|A_{\mathbf{k}}|^2 - |B_{\mathbf{k}}|^2 = 1 \tag{2.17}$$

characteristic of a time-independent canonical transformation. Because of this condition, the Bogoliubov coefficients may be characterized by a hyperbolic angle parameter $\chi_{\mathbf{k}}$. In the second quantized description (2.1) the quantity $|B_{\mathbf{k}}|^2 = \sinh^2 \chi_{\mathbf{k}}$ is the well-defined mean number density of particles at asymptotically late times created in the mode $\mathbf{k}$ by the background electric or gravitational field, assuming the initial vacuum state $|0, in\rangle$. The coefficient $|B_{\mathbf{k}}|^2$ may be calculated in special cases such as the constant E-field and de Sitter space by knowledge of the exact scattering solutions of (2.2) satisfying (2.16), or approximately by the complex WKB adiabatic phase methods to be discussed in the next section, or finally, by direct numerical solution of the mode eq. (2.2).

Since the vacuum state for a non-self-interacting field theory is a product of Gaussian harmonic oscillator wave functions, one for each $\mathbf{k}$, it is a straightforward exercise to represent the initial Gaussian state and Fock space operators in the final state basis, in terms of $|B_{\mathbf{k}}|^2$ or $\chi_{\mathbf{k}}$. For a single real hermitian scalar field beginning in the $|0, in\rangle$ vacuum, the diagonal elements of the

Gaussian density matrix $\hat{\varrho}$ for the n^{th} excited state of the oscillator labelled by $\mathbf{k}$ in the final $|n, out\rangle$ state basis are [46, 47]

$$\hat{\varrho}_n(\mathbf{k})\big|_{\text{Real }\mathbf{\Phi}} = |\langle n, out|0, in\rangle|^2 = \delta_{n,2\ell}\ \frac{(2\ell)!}{4^\ell(\ell!)^2}\ \text{sech}\,\chi_{\mathbf{k}}\,(\tanh\chi_{\mathbf{k}})^{2\ell} \tag{2.18}$$

which in the second quantized Fock space description (2.1), is the probability of finding $n = 2\ell$ particles in the Fourier mode $\mathbf{k}$ in the final state, if none were present in the initial state. In (2.18)

$$\tanh^2\chi_{\mathbf{k}} = \frac{|B_{\mathbf{k}}|^2}{|A_{\mathbf{k}}|^2}\,, \qquad \text{sech}\,\chi_{\mathbf{k}} = \frac{1}{|A_{\mathbf{k}}|} = \left[1 + |B_{\mathbf{k}}|^2\right]^{-\frac{1}{2}} \tag{2.19}$$

with the vanishing of $\hat{\varrho}_n$ for n odd the result of the fact that the particles can only be created in pairs. Thus the probability that no particle pairs at all are produced in any mode,

$$|\langle 0, out|0, in\rangle|^2\big|_{\text{Real }\mathbf{\Phi}} = \prod_{\mathbf{k}} \hat{\varrho}_0(\mathbf{k}) = \prod_{\mathbf{k}} \text{sech}\,\chi_{\mathbf{k}} = \exp\left\{ -\frac{1}{2}\sum_{\mathbf{k}} \ln\left(1 + |B_{\mathbf{k}}|^2\right)\right\} \tag{2.20}$$

is the vacuum persistence probability, or the probability that the $|0, in\rangle$ vacuum at early times will be found in the $|0, out\rangle$ vacuum at late times. Eq. (2.20) relates the probability of vacuum decay directly to particle creation via the number density of created particles $|B_{\mathbf{k}}|^2$ in the final state defined by the one-dimensional scattering problem (2.16) for spatially homogeneous background fields, in the *in-out* formalism of QFT, enforcing the Feynman-Schwinger $m^2 - i\epsilon$ prescription.

For a complex charged scalar field the corresponding diagonal elements of the density matrix are more simply given by [43]

$$\hat{\varrho}_n(\mathbf{k})\big|_{\text{Complex }\mathbf{\Phi}} = |\langle n, out|0, in\rangle|^2 = \delta_{n,2\ell}\ (\text{sech}\,\chi_{\mathbf{k}})^2\,(\tanh\chi_{\mathbf{k}})^{2\ell} \tag{2.21}$$

with (2.19) as before, so that the corresponding vacuum persistence probability is

$$|\langle 0, out|0, in\rangle|^2\big|_{\text{Complex }\mathbf{\Phi}} = \prod_{\mathbf{k}} \hat{\varrho}_0(\mathbf{k}) = \prod_{\mathbf{k}} \text{sech}^2\,\chi_{\mathbf{k}} = \exp\left\{ -\sum_{\mathbf{k}} \ln\left(1 + |B_{\mathbf{k}}|^2\right)\right\} \tag{2.22}$$

for a charged scalar field decaying into pairs [26–29]. The relative factor of 2 between the exponents of (2.20) and (2.22) may be understood as a result of the doubling of degrees of freedom and the one-loop effective action for a complex field relative to a real one. In each case one may check from (2.18) and (2.21) that Tr $\hat{\varrho} = \sum_{\ell=0}^{\infty} \hat{\varrho}_{2\ell} = 1$ so that probability (unitarity) is conserved.

If the external field producing the particles persists over an infinitely long time, homogeneously over an infinite volume, $|B_{\mathbf{k}}|^2$ becomes independent of some components of $\mathbf{k}$, and the sum over $\mathbf{k}$ in (2.20) or (2.22) diverges. This divergence is not a pathology, as is sometimes claimed [40], but simply a consequence of a persistent spatially homogeneous external field producing particles at a finite rate everywhere in space for an infinite time, requiring careful extraction of the volume and

time factors. The spatial volume factor is easily extracted by the usual method of replacing the sum $\sum_{\mathbf{k}}$ over discrete Fourier modes by the continuous Fourier integral $V \int \frac{d^3\mathbf{k}}{(2\pi)^3}$, and dividing the exponent in (2.20),(2.22) by V in the infinite volume continuum limit $V \to \infty$. The vacuum decay rate Γ per unit volume might be defined then by an expression of the form (2.20) or (2.22), with

$$\Gamma = \lim_{T\to\infty} \lim_{V\to\infty} \frac{1}{VT} \frac{N}{2} \sum_{\mathbf{k}} \ln\left(1 + |B_{\mathbf{k}}|^2\right) = \frac{N}{2} \lim_{T\to\infty} \frac{1}{T} \int \frac{d^3\mathbf{k}}{(2\pi)^3} \ln\left(1 + |B_{\mathbf{k}}|^2\right) \tag{2.23}$$

where $N = 1, 2$ refers to the number of independent scalar fields undergoing particle creation, one for a single real field, two for a complex charged scalar. As has been remarked previously [5, 26–28], the integral in (2.23) still diverges for background external fields that persist for an infinite interval of time, and the expression is indeterminate. In order to extract the time factor T, it is necessary either to determine the finite subset or 'window' of Fourier $\mathbf{k}$ modes that experience particle pair creation during specific intervals of time, or alternatively, to apply the external background field only for a *finite* time, compute the Fourier integral, and only at the end take the limit in (2.23).

The first method for defining the decay rate, to be called the Differential (D) Method is suggested by the fact that the integrand $\Gamma = 2\,\mathrm{Im}\,\mathcal{L}_{\mathrm{eff}}$ should be independent of both space and time for persistent external fields of high symmetry. Then one can extract the spacetime volume by identifying the increment of Fourier modes between $\mathbf{k}$ and $\mathbf{k} + \Delta\mathbf{k}$ that undergo their creation events in each small increment of time between t and $t + \Delta t$, in each slice of four-volume between $\mathcal{V}_4$ and $\mathcal{V}_4 + \Delta\mathcal{V}_4$. The determination of which Fourier mode(s) undergo a particle creation 'event' at each time t effectively establishes a functional relation $t = t_{\mathrm{event}}(\mathbf{k})$ or its inverse $\mathbf{k} = \overline{\mathbf{k}}(t)$. Then division by the corresponding four-volume increment gives

$$\Gamma = \frac{N}{2} \lim_{\Delta\mathcal{V}_4\to 0} \frac{1}{|\Delta\mathcal{V}_4|} \sum_{\mathbf{k}}^{\mathbf{k}+\Delta\mathbf{k}} \ln\left(1 + |B_{\mathbf{k}}|^2\right) = \frac{N}{2} \frac{V}{(2\pi)^3} \int \left|\frac{d^3\mathbf{k}}{d\mathcal{V}_4}\right| \ln\left(1 + |B_{\mathbf{k}}|^2\right)\Big|_{\mathbf{k}=\overline{\mathbf{k}}(t)} \tag{2.24}$$

for the decay rate in the presence of the persistent background field, due the increment of Fourier modes going through their pair creation events in an incremental slice of four-volume $d\mathcal{V}_4$ at t, in the limit that both these increments are infinitesimal. There is then no infinite T to be considered and the $\mathbf{k}$ integration in (2.24) is to be performed restricted to only those Fourier modes experiencing a particle creation event at the time $t = t_{\mathrm{event}}(\mathbf{k})$, while the values of $|B_{\mathbf{k}}|^2$ to be used are determined by the asymptotic scattering problem (2.16) for the persistent external field.

The characterization of the particle creation 'event' needed in the Differential Method is the semi-classical event time, $t_{\mathrm{event}}(\mathbf{k})$ and thence its inverse $\mathbf{k} = \overline{\mathbf{k}}(t)$ is based upon the behavior of the adiabatic phase integral (2.9) in the complex time domain, and in particular by the pattern of Stokes and anti-Stokes lines of constant Real and Imaginary parts of $\Theta_{\mathbf{k}}$ emanating from the

complex critical points in t at which $\omega_{\mathbf{k}}^2$ vanishes. The particle creation 'event' is then associated with the time $t_{\rm event}(\mathbf{k})$ at which the Stokes' line for a given $\mathbf{k}$ crosses the real time axis. At this time the amplitude of the antiparticle complex conjugate mode function $f_{\mathbf{k}}^{(0)*}$ rises rapidly [5]. Determining the finite subset of Fourier modes that experience a particle creation 'event' in the finite time interval in this way determines a finite range in the Fourier integral in (2.23) proportional to dt, which allows the finite rate Γ to be determined by (2.24), by computing the indicated (positive) Jacobian $|d^3\mathbf{k}/d\mathcal{V}_4|$.

In the second method for defining the decay rate, to be called the Integral (I) Method, one replaces the persistent background field of interest, such as de Sitter space which extends infinitely far into the past and future, and which is responsible for the divergent $\mathbf{k}$ integral, by a substitute external background field which is turned on slowly around some initial time t_0, persists for a very long but *finite* time T, and then is turned off again slowly at a later time t_1. Since for any fixed finite T only a finite range of Fourier modes will undergo particle creation events, $|B_{\mathbf{k}}^2|$ will vanish rapidly outside of a finite window in Fourier space and the integral over $\mathbf{k}$ in (2.23) will be finite, but proportional to T. Then one can divide by T and explicitly take the $T \to \infty$ limit indicated in (2.23) to obtain a finite result for the vacuum decay rate.

This Integral Method has the advantage of defining zero field regions in the infinite past ($t \ll t_0$) and infinite future ($t \gg t_1$) where particles and vacuum states are unambiguously defined by the standard flat Minkowski space prescription (2.7)-(2.8). However for this method to work, it is essential that a suitable substitute time-dependent external field be found for which the turning on and off of the background of interest around t_0 and t_1 be gentle enough not itself to create significant numbers of particles by violation of the adiabatic condition (2.14), *and* for which any 'edge effects' of particle creation around t_0 and t_1 become negligible in the long time limit $T \to \infty$.

When these criteria are satisfied the Integral Method should give the same result as the Differential Method for defining the decay rate of the vacuum in a (nearly) constant external field, since the long-time time average of a constant integrand is the constant integrand itself. An example of an external field time profile satisfying these criteria and application of the Integral Method to the uniform E-field case is provided by (4.7), shown in Fig. 4, with the result of Sec. IV for the vacuum decay rate agreeing with Schwinger's result in the limit $T \to \infty$. In this flat space example VT is simply the total four-volume $\int d^4x = \mathcal{V}_4$ over which the external E-field acts, and $\Gamma = 2\,\mathrm{Im}\,\mathcal{L}_{\rm eff}$ at one-loop order in Schwinger's approach.

These general considerations and both methods of defining the vacuum decay rate are best illustrated with specific examples. In this paper we apply both methods to the cases of particle

creation in a constant, uniform electric field and in the gravitational de Sitter background. After first reviewing the persistent field calculation of the vacuum decay and particle creation, and the complex adiabatic phase for analyzing particle creation in real time, we present numerical results for the adiabatic switching on and off again of each background after a long time T, and comparison of the vacuum decay rate Γ computed by both the Differential and Integral Method in each case.

III. PERSISTENT UNIFORM ELECTRIC FIELD BACKGROUND

The constant, uniform electric field has been studied by numerous authors by a variety of methods [3, 5, 6, 25–29], and may be considered the prototype of the class of problems involving particle creation and quantum vacuum decay of classically persistent fields. Choosing the time dependent gauge

$$A_z = -Et\,, \qquad A_t = A_x = A_y = 0 \tag{3.1}$$

the Klein-Gordon eq. for a charged scalar field may be separated in Fourier modes as in (2.1) with

$$\omega^2_{\mathbf{k}}(t) = (k_z + eEt)^2 + k_\perp^2 + m^2\ . \tag{3.2}$$

We then obtain the mode equation

$$\left[\frac{d^2}{du^2} + \frac{u^2}{4} + \lambda\right] f_\lambda(u) = 0 \tag{3.3}$$

in the dimensionless time and transverse momentum variables

$$u \equiv \sqrt{\frac{2}{|eE|}}\,\Big(k_z + eEt\Big)\,, \qquad \lambda \equiv \frac{k_\perp^2 + m^2}{2\,|eE|} > 0 \tag{3.4}$$

with $f_{\mathbf{k}}(t)$ relabelled as $f_\lambda(u)$. One immediately observes that the frequency function (3.2) is strictly positive everywhere on the real time axis, for $m^2 > 0$.

The function $\delta_{\mathbf{k}}$ entering the adiabatic condition (2.14) in this case is

$$\delta_\lambda(u) = \frac{1}{2}\,\frac{(3u^2 - 8\lambda)}{(u^2 + 4\lambda)^3} \tag{3.5}$$

from which some properties of particle creation in an electric field background can already be deduced. First one notices that

$$\delta_\lambda(u) \to \frac{3}{2u^4} \to 0 \qquad \text{as} \qquad u \to \mp\infty \tag{3.6}$$

for *any* λ or $\mathbf{k}$. Thus the adiabatic condition (2.14) is asymptotically satisfied for the persistent, strictly constant and uniform electric field, in both the $t \to \mp\infty$ limits, and asymptotic $|0, in\rangle$ and $|0, out\rangle$ vacuum states exist in which the solutions of (3.3) approach (2.10) and its complex

conjugate arbitrarily accurately. This implies in turn that the scattering problem (2.16) is well-posed, and the Bogoliubov coefficients $B_{\mathbf{k}}$ are finite and well-defined for each $\mathbf{k}$.

In fact the exact solutions of (3.3) are parabolic cylinder functions, whose asymptotic behaviors and analytic properties are well known. From these solutions and properties one finds [5, 26–28]

$$B_{\mathbf{k}} = -ie^{-\pi\lambda} = -i\,\exp\left\{-\frac{\pi}{2}\,\frac{k_\perp^2+m^2}{|eE|}\right\} \tag{3.7}$$

exactly, for any $\lambda > 0$. As anticipated by our general discussion in the last section, if this value is substituted into (2.23) we obtain an indeterminate result, since $|B_{\mathbf{k}}|^2$ is independent of k_z and the integral over k_z in (2.23) is linearly divergent. This is clearly associated with the fact that the parallel component of the conserved (canonical) momentum k_z enters the mode eq. (3.3) together with the time t only through the gauge invariant combination $k_z + eEt \equiv p_z(t)$, which is the physical kinetic momentum, so that a linear divergence in k_z is associated with the infinite time in which the E-field is applied in obtaining (3.7).

Now from (3.5) the maximum violation of the adiabaticity condition (2.14) is

$$\max\left\{|\delta_\lambda(u)|\right\} = \frac{1}{16\lambda^2} \qquad \text{at} \qquad u=0, \quad p_z(t) = k_z + eEt = 0 \tag{3.8}$$

so that the time at which this maximum violation occurs is the time

$$t_{\text{event}}(k_z) = -\frac{k_z}{eE} \;\Rightarrow\; \overline{k}_z(t) = -eEt \tag{3.9}$$

when a mode of a given k_z has zero kinetic momentum along the field. By symmetry of (3.3) under $u \to -u$ we may expect that (3.9) is the time which may be identified with a creation 'event' in the mode with longitudinal canonical momentum k_z, and $\overline{k}_z(t)$ denotes the value of k_z of the Fourier mode experiencing its creation event at time t. Eq. (3.9) is the relation between k_z and the time of particle creation that allows the Jacobian factor

$$\left|\frac{d^3\mathbf{k}}{d\mathcal{V}_4}\right|_{\mathbf{k}=\overline{\mathbf{k}}(t)} = \frac{d^2\mathbf{k}_\perp}{V}\left|\frac{d\overline{k}_z}{dt}\right| = \frac{|eE|}{V}\,d^2\mathbf{k}_\perp \tag{3.10}$$

appearing in (2.24) to be computed, eliminating any integral over k_z, while the value of $\mathbf{k}_\perp$ is unrestricted and must still be integrated over to give a well-defined result for the vacuum decay rate by the Differential Method (2.24). The absolute value must be taken for the Jacobian in order for a positive increment in dk_z to correspond to a positive increment in time dt for $eE > 0$, which we may assume henceforth with no loss of generality.

The maximal violation of adiabaticity at $u = 0$ in (3.8) goes to zero as $\lambda \to \infty$. so that, as expected, heavier particles with larger transverse momenta are more difficult to create, however

falling only as a power λ^{-2} for large λ, whereas the actual asymptotic value of the created particles in the mode specified by λ falls exponentially with λ, *cf.* (3.7). The contrast between the λ^{-2} power of the maximum of $|\delta_\lambda(u)|$ *vs.* the exponential λ dependence of $B_{\mathbf{k}}$ illustrates the distinction between local or transient violations of (2.14) *vs.* global or secular particle creation effects which persist at late times.

The asymptotic value of the Bogoliubov coefficients in (2.16) can be obtained by consideration of the global analyticity properties of the solutions of (3.3), or in the WKB approximation by the behavior of the adiabatic phase (2.9) in the complex time domain [48–50]. The adiabatic phase (2.9) expressed in dimensionless u, λ variables is

$$\Theta_\lambda(u) = \frac{1}{2}\int_0^u du\,\sqrt{u^2+4\lambda} = \frac{u}{4}\sqrt{u^2+4\lambda} + \lambda \ln\left(\frac{u+\sqrt{u^2+4\lambda}}{2\sqrt{\lambda}}\right) \tag{3.11}$$

in this case, when measured from the symmetric point at $u = 0$. Since $\omega_k^2 = eE(u-u_\lambda)(u+u_\lambda)/2$ has two isolated zeroes in the complex domain, at

$$u = \pm u_\lambda = \pm 2i\sqrt{\lambda} \tag{3.12}$$

where $\omega_{\mathbf{k}}^2$ vanishes linearly, linear turning point WKB methods may be applied in the complex domain. From each linear turning point three Stokes lines (of constant Real Θ_λ) and three anti-Stokes lines (of constant Imaginary Θ_λ) emerge, at 60° to each other. The solution of the mode eq. (3.3) that has the asymptotic limits (2.16) may be found by analytic continuation in the upper half complex u plane along the solid anti-Stokes lines of constant Im $\Theta_\lambda(u)$ illustrated in Fig. 1.

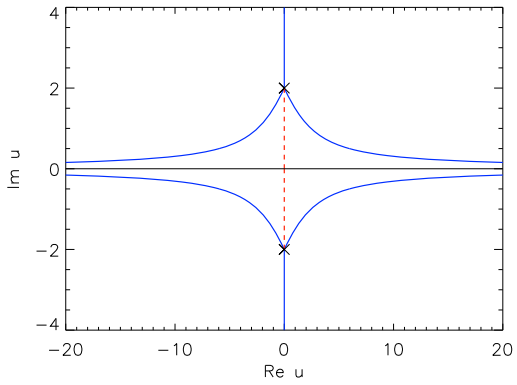

FIG. 1. The solid (blue) lines are the three anti-Stokes lines of constant Im Θ_λ emerging from the two complex zeroes (3.12) of (3.2). The dashed (red) line is the Stokes line of constant Re Θ_λ connecting the two critical points, which crosses the real axis at $u = 0$, defining the time (3.9) of the particle creation event.

The square root and logarithm in (3.11) are defined as the analytic continuation from the real axis of their principal value everywhere in the complex u plane, cut by the branch cut taken to be along the positive and negative imaginary axes for $|u| > 2\sqrt{\lambda}$. The constant Im Θ_λ of the phase

function along its anti-Stokes lines in the upper half plane is given by its value at the critical point $+u_\lambda$,

$$\mathrm{Im}\,\Theta_\lambda(u_\lambda) = \mathrm{Im}\left[\lambda \ln(i)\right] = \frac{\pi\lambda}{2} \tag{3.13}$$

and the adiabatic mode function (2.10) is a good approximation to the exact solution everywhere along the u contour defined by the solid blue anti-Stokes line in the upper half-plane, except in the vicinity of the complex turning point $u = u_\lambda$. There a standard WKB linear turning point analysis and matching of the asymptotic solutions on the two halves of the anti-Stokes contour determines

$$B_\lambda = -i \exp\left[-2\,\mathrm{Im}\,\Theta_\lambda(u_\lambda)\right] = -i\, e^{-\pi\lambda} \tag{3.14}$$

which coincides with the exact value (3.7) in this simple example of only one linear complex critical point in the upper half u-plane.

The number density of particles in momentum $\mathbf{k}$ as $t \to \infty$, if started in the initial state vacuum at $t \to -\infty$ is therefore

$$|B_\lambda|^2 = \exp\left[-4\,\mathrm{Im}\,\Theta_\lambda(u_\lambda)\right] = e^{-2\pi\lambda} = \exp\left[-\frac{\pi(k_\perp^2 + m^2)}{eE}\right] \tag{3.15}$$

and the solutions of the mode eq. (3.3) exhibit a fairly sharp transition, illustrated in Fig. 2, from the early to late time asymptotic forms (2.16) at $u = 0$ where the Stokes line of constant Re Θ_λ crosses the real time axis at $u = 0$ in Fig. 1.

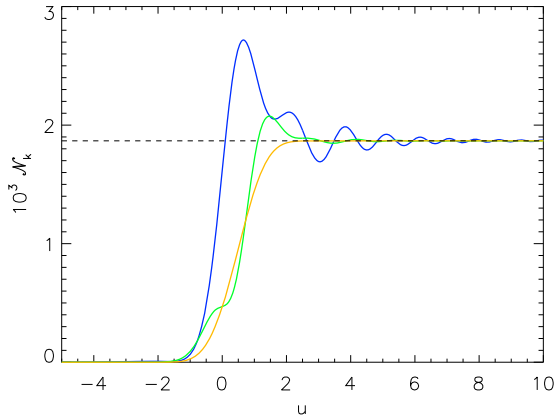

FIG. 2. The mean number of particles created from the vacuum by a constant, uniform electric field as a function of rescaled time u, for $\lambda = 1$. The first two curves (blue and green) are the adiabatic particle numbers $\mathcal{N}_{\mathbf{k}}^{(n)}$, defined by (2.15) for $n = 1, 2$ with $f_{\mathbf{k}} = f_{\lambda\,(+)}(u)$ the *in*-state solution of (3.3), given by Eqs. (4.9a) and (5.11)-(5.13) of Ref. [5]. The third curve (orange) with no intermediate maxima and minima is the 'superadiabatic' particle number (3.16) [51, 52]. Apart from transient effects dependent on the adiabatic order, all three curves rise rapidly from zero in the vicinity of $u = 0$ and tend to the same asymptotic value $e^{-2\pi} = 1.86744 \times 10^{-3}$ of (3.15) as $u \to \infty$.

The particle creation event is defined by the rapid rise in adiabatic particle number defined by (2.15), together with Eqs. (4.9a) and (5.11)-(5.13) of Ref. [5], and illustrated in Fig. 2.[2] For comparison the universal, optimally adiabatic, or *'superadiabatic'* particle number $\overline{\mathcal{N}}_\lambda$ [51, 52], given in terms of the adiabatic phase integral by

$$\overline{\mathcal{N}}_\lambda(u) = \frac{1}{4}\exp\big[-4\,\mathrm{Im}\,\Theta_\lambda(u_\lambda)\big]\left\{\mathrm{erfc}\left[\frac{-\Theta_\lambda(u)}{\sqrt{\mathrm{Im}\,\Theta_\lambda(u_\lambda)}}\right]\right\}^2 = \frac{e^{-2\pi\lambda}}{4}\left\{\mathrm{erfc}\left[-\sqrt{\frac{2}{\pi\lambda}}\,\Theta_\lambda(u)\right]\right\}^2 \quad (3.16)$$

is also shown in Fig. 2 for the E-field. The time of the event at $u = 0$ coincides in this case with the maximum value of $|\delta_\lambda(u)|$, (3.8). Apart from non-universal transients illustrating the quantum uncertainty in defining particle number at the transition, which depend upon the adiabatic order of particle number definition, the particle creation event is characterized by a permanent secular rise (3.15). This asymptotic particle number is unambiguously defined and independent of adiabatic order, but exponentially small in λ for large λ, and can be obtained from the global analysis of the adiabatic phase (3.11), and its critical point u_λ (3.12) in the complex time domain.

This detailed description of the Stokes' lines of the adiabatic phase and time (3.9) when each k_z mode goes through its creation event determines the Jacobian factor (3.10) in the differential rate formula (2.24) for the constant E-field background. Equivalently it also informs us how to regulate the k_z integral in a finite time T in the integral formula (2.23). For if one starts in the adiabatic vacuum with mode function (2.10) for all modes at some *finite* initial time t_0, one sees from (3.8) and (3.9) that only those modes for which

$$p_z(t_0) < 0 :\ t_{\mathrm{event}}(k_z) > t_0 \qquad \text{but} \qquad p_z(t_1) > 0 :\ t_{\mathrm{event}}(k_z) < t_1 \quad (3.17)$$

experience their particle creation event between t_0 and t_1. Thus we may approximate

$$|B_{\mathbf{k}}|^2 \simeq \begin{cases} e^{-2\pi\lambda} & \text{for} \quad -eEt_1 < k_z < -eEt_0 \\ 0 & \text{otherwise} \end{cases} \quad (3.18)$$

and in the finite elapsed time $T = t_1 - t_0$ only modes in the k_z interval of the window linearly growing in time in (3.18) give a non-vanishing contribution to the vacuum decay rate. With the step function approximation of (3.18) and (2.23) then yield

$$\begin{aligned}\Gamma &= \lim_{T\to\infty}\frac{1}{T}\int_{-eEt_1}^{-eEt_0}\frac{dk_z}{2\pi}\int\frac{d^2\mathbf{k}_\perp}{(2\pi)^2}\,\ln\left(1+e^{-2\pi\lambda}\right) \\ &= \frac{eE}{2\pi}\int\frac{d^2\mathbf{k}_\perp}{(2\pi)^2}\,\ln\left\{1+\exp\left[-\frac{\pi\,(k_\perp^2+m^2)}{eE}\right]\right\}\end{aligned}$$

[2] The first line of Eq. (5.13) of Ref. [5] contains a typographical error in its last term which should read $\frac{3}{8}\frac{\dot\omega_{\mathbf{k}}^2}{\omega_{\mathbf{k}}^3}$.

$$= \frac{eE}{2(2\pi)^2}\int_0^\infty dk_\perp^2 \sum_{n=1}^\infty \frac{(-)^{n+1}}{n}\exp\left[-\frac{\pi n\,(k_\perp^2+m^2)}{eE}\right]$$
$$= \frac{(eE)^2}{(2\pi)^3}\sum_{n=1}^\infty \frac{(-)^{n+1}}{n^2}\exp\left(-\frac{\pi n m^2}{eE}\right) \tag{3.19}$$

which agrees with Schwinger's proper time method for the calculation of the decay rate of a uniform electric field into scalar particle/antiparticle pairs [25]. Clearly the identical expression is obtained from the Differential Method (2.24) upon making use of (3.10) which eliminates the k_z integral, T dependence and limit entirely, giving directly the second line of (3.19). We next verify (3.19) by turning the E-field on and off adiabatically, letting it last for a very long time T and extrapolating to the limit indicated in the Integral Method (2.23) numerically.

IV. ADIABATIC SWITCHING ON/OFF OF A UNIFORM ELECTRIC FIELD

Before discussing the E-field profile needed to compute the vacuum decay rate by the Integral Method, we mention first the modified E-field time profile

$$\mathbf{E}(t) = E\,\hat{\mathbf{z}}\,\mathrm{sech}^2\,(t/T) \tag{4.1}$$

that has been considered in the literature [30, 53], for which the electric field vanishes asymptotically in both the $t \to \mp\infty$ limits. This corresponds to the spatially uniform gauge potential

$$A_z(t) = -ET\tanh\,(t/T) \tag{4.2}$$

for which the mode eq. (2.2) with

$$\omega_{\mathbf{k}}^2(t) \equiv \left[k_z + eET\tanh\,(t/T)\right]^2 + k_\perp^2 + m^2 \tag{4.3}$$

may be solved exactly in terms of hypergeometric functions [30, 53]. The frequency has the asymptotic limits

$$\lim_{t\to\pm\infty}\omega_{\mathbf{k}}(t) \equiv \omega_{\mathbf{k}}^\pm = \sqrt{(k_z \pm eET)^2 + k_\perp^2 + m^2} \tag{4.4}$$

which are constants. Thus the positive frequency particle and negative frequency antiparticle modes are the unique zero-field modes in each asymptotic limit. From the analytic properties of the exact hypergeometric function solutions of the mode equation (2.2) with (4.3), the Bogoliubov coefficients of the scattering problem (2.16) may also be computed analytically, with the result [28, 30, 53]

$$|A_{\mathbf{k}}(T)|^2 = \frac{\cosh^2\left[\frac{\pi}{2}\sqrt{(2eET^2)^2-1}\right] + \sinh^2\left[\frac{\pi}{2}\,(\omega_{\mathbf{k}}^+ + \omega_{\mathbf{k}}^-)\,T\right]}{\sinh(\pi\omega_{\mathbf{k}}^+ T)\ \sinh(\pi\omega_{\mathbf{k}}^- T)} \tag{4.5a}$$

$$|B_{\mathbf{k}}(T)|^2 = \frac{\cosh^2\left[\frac{\pi}{2}\sqrt{(2eET^2)^2-1}\right] + \sinh^2\left[\frac{\pi}{2}\left(\omega_{\mathbf{k}}^+ - \omega_{\mathbf{k}}^-\right)T\right]}{\sinh(\pi\omega_{\mathbf{k}}^+ T)\ \sinh(\pi\omega_{\mathbf{k}}^- T)} \tag{4.5b}$$

satisfying (2.17) for all $\mathbf{k}$ and T.

The Bogoliubov coefficient $|B_{\mathbf{k}}(T)|^2$ is well-behaved as $|k_z| \to \infty$ (T fixed), being proportional to $\exp(-2\pi|k_z|T)$ and vanishing exponentially in that limit. Hence for any finite T the integral over k_z and the total number of particles created is finite. In the opposite limit, with k_z fixed

$$\lim_{T\to\infty} |B_{\mathbf{k}}(T)|^2 = \exp\left(-\pi\,\frac{k_\perp^2 + m^2}{eE}\right) = e^{-2\pi\lambda} \tag{4.6}$$

the value in the constant electric field (3.15) independent of k_z is recovered. Thus the large k_z and large T limits of (4.5b) do not commute. The behavior of $|B_{\mathbf{k}}(T)|^2$ as a function of k_z and of T is shown in Figs. 3, with the flattening for small $|k_z|$ as $T \to \infty$ according to (4.6) illustrated.

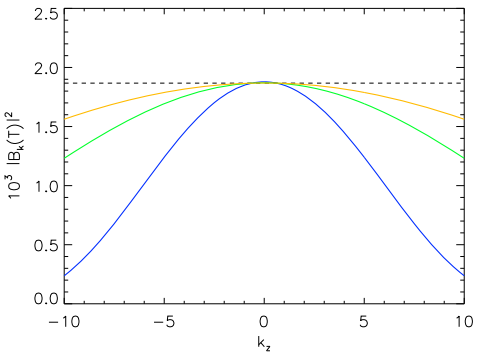

FIG. 3. Particle Density $|B_{\mathbf{k}}(T)|^2$ of (4.5b) for the E-field (4.1), as a function of $k_z/\sqrt{eE}$ for $\lambda = 1$. The curve that falls off the most rapidly in $|k_z|$ (blue) is for $\sqrt{eE}\,T = 20$, the middle one (green) is for $\sqrt{eE}\,T = 40$, and the outer one (orange) is for $\sqrt{eE}\,T = 60$, showing the approach to $e^{-2\pi\lambda}$ (dashed line) near $k_z = 0$.

The time profile (4.1) *cannot* be used to compute the decay rate of a constant E-field by the Integral Method (2.23), because the E-field (4.1) is not constant over times of order T. Although the turning on and off of the E-field in (4.1) is adiabatic, the time for the transition also grows with T and hence as Fig. 3 shows, the particle production (4.5b) falls off smoothly in $|k_z|$, rather than sharply outside a well-defined window in k_z, as required to match the flat plateau behavior (3.18) for a constant E-field. However we may extract the constant E-field Schwinger rate from (4.1)-(4.6) through the Differential Rate formula (2.24), provided we compute the Jacobian (3.10), restricted to finite values of k_z in the limit $T \to \infty$, where (4.6) holds, corresponding to finite times $|t| \ll T$ when the E-field (4.1) is constant. In that limit because of (4.6) and making use of the Jacobian (3.10) based on the constant E limit, the second line of (3.19) and finally Schwinger's vacuum decay rate for a constant E-field is recovered.

In order to use the Integral Method (2.23) one needs instead at least a *two*-parameter family of time profiles in which the parameter controlling the duration of the field is separate and distinct from the parameter controlling the time during which the field is switched on and off again. An analytical function with these properties is

$$\mathbf{E}(t) = \frac{E\,\hat{\mathbf{z}}}{2}\Big\{\tanh\left[b\,(t-t_0)\right] - \tanh\left[b\,(t-t_1)\right]\Big\} \tag{4.7}$$

some examples of which are shown in Fig. 4. This profile has the property that $E(t)$ vanishes well before some initial time t_0 and well after some final time t_1 where $t_1 - t_0 \equiv T > 0$. Now T can be taken arbitrarily large, while $\mathbf{E}(t)$ has approximately the constant value $E\,\hat{\mathbf{z}}$ between t_0 and t_1, and is adiabatically switched on and off on an arbitrary time scale of order b^{-1}: *cf.* Fig. 4. Thus if b is small enough, the particle creation during the adiabatic switching on and off of the E-field may be kept small, and rendered negligible compared to the particle creation during the arbitrarily long interval of time T when the field is constant.

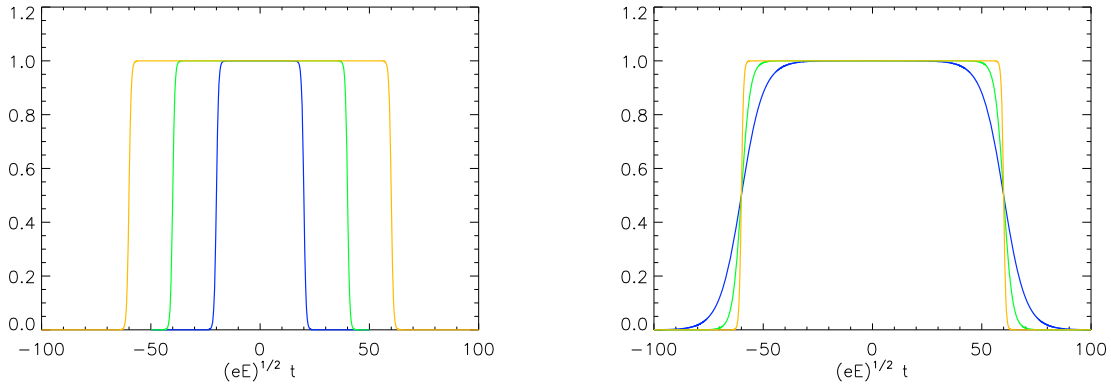

FIG. 4. The electric field for the profile (4.7) in units of its maximum as a function of time with $t_1 = -t_0$. The curves in the Left Panel show fixed $b/\sqrt{eE} = 1$, with $\sqrt{eE}\,t_1 = 20$ (blue), 40 (green), 60 (orange). The curves in the Right Panel show fixed $\sqrt{eE}\,t_1 = 60$ with $b/\sqrt{eE} = 0.1$ (blue), 0.25 (green), 1 (orange).

The gauge potential corresponding to (4.7) may be taken to be

$$A_z(t) = -\frac{E}{2b}\,\ln\left\{\frac{\cosh\left[b\,(t-t_0)\right]}{\cosh\left[b\,(t-t_1)\right]}\right\} - \frac{E(t_0+t_1)}{2} \tag{4.8}$$

which behaves as

$$A_z(t) \simeq -E\begin{cases} t_0 & t \ll t_0 \\ t & t_0 \ll t \ll t_1 \\ t_1 & t_1 \ll t \end{cases} \tag{4.9}$$

for $b(t_1 - t_0) = bT \gg 1$. For this potential no analytic solution for the mode eq. (2.2) is known and we must rely on a numerical solution. The Bogoliubov coefficients $|B_{\mathbf{k}}|^2$ are finite as is the integral over all modes, and the decay rate is now computed by the Integral Method (2.23), taking

the $T \to \infty$ limit numerically. The numerical results for the integrand $\ln(1 + |B_{\mathbf{k}}|^2)$ shown in Fig. 5 (unlike Fig. 3) now show the expected linear opening of the approximately constant window function in k_z as $T = t_1 - t_0$ is increased.

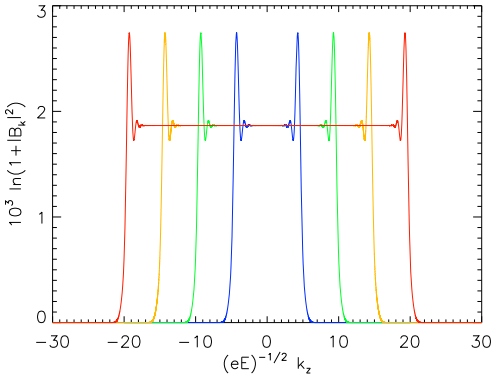

FIG. 5. The numerically computed integrand $\ln(1 + |B_{\mathbf{k}}|^2)$ for the rate as a function of k_z for four different values of t_1 when $\lambda = b/\sqrt{eE} = 1$ and $t_0 = -t_1$. Going out from $k_z = 0$ in either direction the curves correspond to $\sqrt{eE}t_1 = 10$ (blue), 20 (green) 30 (orange), and 40 (red).

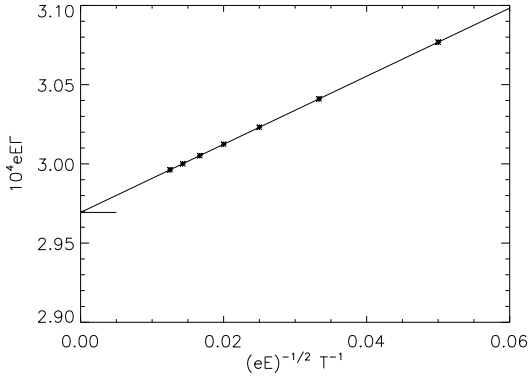

FIG. 6. The two dimensional rate (4.10) as a function of T^{-1} for the case $\lambda = b/\sqrt{eE} = 1$. The crosses are our numerical data. The solid line going through them is a least squares fit to the data which is extrapolated to $T^{-1} \to 0$. The horizontal line segment gives the value of the rate for this value of λ when the electric field is static, according to the Schwinger formula (3.19), to which the numerical results extrapolate.

For a uniform E-field in two spacetime dimensions, dropping the transverse $d^2\mathbf{k}_\perp/(2\pi)^2$ integral, the Integral Rate (2.23) is

$$\Gamma_{2D} = \lim_{T\to\infty} \frac{1}{T} \int_{-\infty}^{\infty} \frac{dk_z}{2\pi} \ln(1 + |B_{\mathbf{k}}|^2) \,. \tag{4.10}$$

which is shown as a function of T in Fig. 6, with the limit extrapolated to the Schwinger result in $d = 2$ for $T^{-1} = 0$. The linear fit to the $1/T$ extrapolation shows that the finite edge effects and particle creation due to the switching on and off of the E-field around $t = t_0$ and $t = t_1$ remain finite while the constant E-field contribution to (4.10) increases linearly as the time interval T increases.

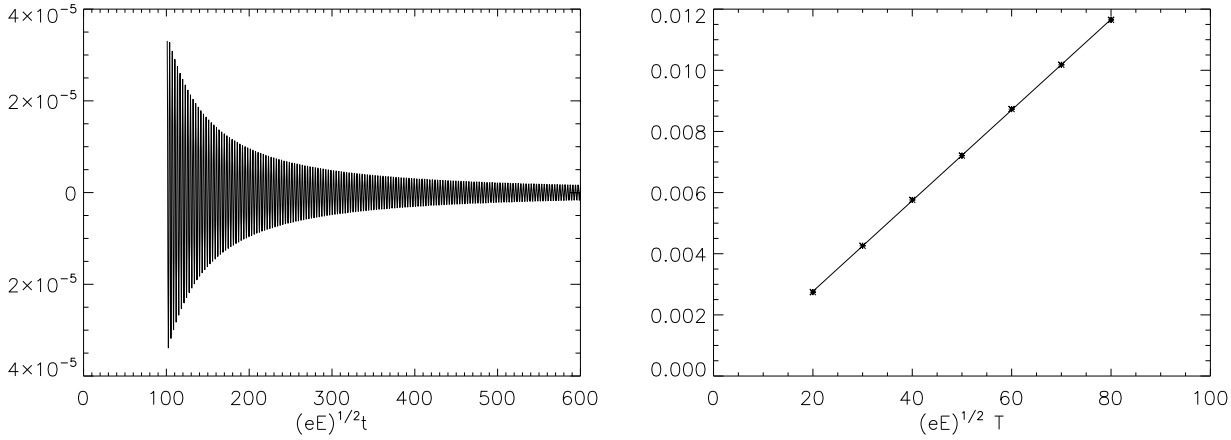

FIG. 7. Left Panel: The oscillating $A_{\mathbf{k}}B^*_{\mathbf{k}}$ part of the current (4.11) with $\lambda = 1$ as a function of time for the case $t_1 = -t_0 = 30(eE)^{-1/2}$ corresponding to $T = 60(eE)^{-1/2}$, showing that it averages to zero and that its oscillations are damped at late times after the E-field is turned off. Right Panel: The constant non-oscillating $|B_{\mathbf{k}}|^2$ particle contribution to the current (4.11) with $\lambda = 1$ at late times, as a function of the time T for which the E-field was turned on. The solid line is a linear T fit to the numerical data.

The electric current from the created charged particle pairs at the end of the process, *i.e.* at late times after the electric field has been turned off, is easily evaluated. In this case, the vacuum-subtracted z component of the electric current the two-dimensional case at late times is [43]

$$\begin{aligned}\langle j_z\rangle\Big|_{d=2} &= 2e\int_{-\infty}^{\infty}\frac{dk_z}{2\pi}\,(k_z - eA_z)\left[|f_{\mathbf{k}}(t)|^2 - \frac{1}{2\omega_{\mathbf{k}}}\right] \\ &= 2e\int_{-\infty}^{\infty}\frac{dk_z}{2\pi}\,\frac{(k_z - eA_z)}{\omega_{\mathbf{k}}}\left[|B_{\mathbf{k}}|^2 + \mathrm{Re}\left(A_{\mathbf{k}}B^*_{\mathbf{k}}e^{-i\omega_{\mathbf{k}}t}\right)\right] \to 2e\int_{-\infty}^{\infty}\frac{dk_z}{2\pi}\,\frac{(k_z - eA_z)}{\omega_{\mathbf{k}}}\,|B_{\mathbf{k}}|^2 \qquad (4.11)\end{aligned}$$

which contains a non-oscillating constant $|B_{\mathbf{k}}|^2$ term from the created particles, as well as a rapidly oscillating quantum interference $A_{\mathbf{k}}B^*_{\mathbf{k}}$ term. The latter gives rise to a rapidly oscillating transient contribution that decays away with time due to phase cancellations (Left Panel of Fig. 7). In contrast the contribution from the created particles gives a constant contribution to the current at late times, whose value depends linearly upon the total time T during which the electric field was applied, as expected from the linerarly opening window in k_z (Right Panel of Fig. 7). This linear growth with T shows that the backreaction of the current of the particles created by a persistent electric field must eventually be taken into account, no matter how small the coupling e [54].

V. VACUUM DECAY OF DE SITTER SPACE: FLAT SPATIAL SECTIONS

The globally complete closed $\mathbb{S}^3$ spatial sections and contracting part of de Sitter space have been considered in detail in [5, 6], showing that global de Sitter space is unstable to particle creation, with exponentially growing energy density. Here we specialize to the flat spatial sections

of spatially homogeneous and isotropic Friedman-Lemaitre-Robertson-Walker (FLRW) spacetimes with the metric line element

$$ds^2 = -dt^2 + a^2(t)\, d\mathbf{x}^2 \tag{5.1}$$

presumed most relevant for cosmology. In the FLRW background geometry (5.1) the scalar wave eq. $(-\Box + m^2 + \xi R)\Phi = 0$ (with R the scalar curvature) separates. Hence the scalar field may be represented as a Fourier sum analogous to (2.1), with mode solutions of the form $\Phi \sim \phi_k(t) e^{i\mathbf{k}\cdot\mathbf{x}}$. Removing the scale factor by defining the complex mode function $f_k(t) = a(t)^{\frac{3}{2}}\phi_k(t)$ gives a mode equation for $f_k(t)$ which is again of the form (2.2) with a time dependent frequency

$$\omega^2_{\mathbf{k}}(t) = \frac{\mathbf{k}^2}{a^2} + m^2 - \frac{h^2}{4} - \frac{\dot{h}}{2} + (6\xi - 1)(2h^2 + \dot{h}) \tag{5.2}$$

where $h \equiv \dot{a}/a$ for general $a(t)$. We consider here the case of conformal coupling $\xi = \frac{1}{6}$ to simplify the algebra, although the same methods may be applied for any ξ. For de Sitter space $a(t) = a_{\rm dS}(t) = \exp(Ht)$, with $h = H$ a constant and $\dot{h} = 0$. Then defining the dimensionless time variable $u \equiv Ht$ and dimensionless momentum $k \equiv |\mathbf{k}|/H$, the oscillator equation (2.2) becomes

$$\left[\frac{d^2}{du^2} + \omega^2_{k\gamma}(u)\right] f_{k\gamma}(u) = 0 \tag{5.3}$$

with the time dependent dimensionless frequency function given by

$$\omega^2_{k\gamma}(u) = k^2 e^{-2u} + \gamma^2 \qquad \text{and with} \qquad \gamma \equiv \sqrt{\frac{m^2}{H^2} - \frac{1}{4}}\,. \tag{5.4}$$

We restrict ourselves here to the massive case $m^2 > H^2/4$, in the principal series spin-0 representation of the $SO(4,1)$ de Sitter isometry group [55], so that γ is real and positive, as is $\omega^2_{k\gamma}(u)$.

The adiabatic parameter appearing in (2.14) in this case is

$$\delta_{k\gamma}(u) = \frac{k^2 e^{-2u}}{8\,\omega^6_{k\gamma}}\,\left(k^2 e^{-2u} - 4\gamma^2\right) = \frac{1}{8\,\omega^2_{k\gamma}}\left(1 - \frac{\gamma^2}{\omega^2_{k\gamma}}\right)\left(1 - \frac{5\,\gamma^2}{\omega^2_{k\gamma}}\right) \tag{5.5}$$

which reveals that as in the E-field case (3.6), so also in de Sitter space

$$\lim_{u\to\mp\infty} \delta_{k\gamma}(u) = 0 \qquad \text{for every} \quad k, \gamma \geq 0\,. \tag{5.6}$$

Hence there is a well-defined adiabatic $|0, in\rangle$ and $|0, out\rangle$ vacuum state asymptotic in each infinite time limit of de Sitter space, the scattering problem (2.16) is again well-posed, and the Bogoliubov coefficients $B_{\mathbf{k}}$ finite and well-defined for every $\mathbf{k}$. In between the asymptotic limiting times (5.6), at a finite u of order $\ln(k/\gamma)$ the absolute value of $|\delta_{k\gamma}|$ attains the maximum

$$\max|\delta_{k\gamma}| \simeq \frac{0.0656423}{\gamma^2} \tag{5.7}$$

which may be compared to (3.8) in the E-field case.

Determining the correct magnitude of the secular particle creation effect and its detail in real time again requires a global analysis of the adiabatic phase integral in the complex time domain. Changing variables to the physical momentum (in units of H)

$$z \equiv \frac{k}{a} = k\, e^{-u} \tag{5.8}$$

so that $\omega_{k\gamma} = \sqrt{z^2+\gamma^2}$, one finds the adiabatic phase integral

$$\begin{aligned}\Theta_\gamma(z) &\equiv \int_{u_{k\gamma}}^{u(z)} du\ \omega_{k\gamma}(u) = -\int_{\gamma\kappa}^{z} \frac{dz}{z}\sqrt{z^2+\gamma^2} \\ &= -\sqrt{z^2+\gamma^2} + \gamma \ln\left[\frac{\sqrt{z^2+\gamma^2}+\gamma}{z}\right] \to \begin{cases} -z & z\to\infty \\ -\gamma\ln z & z\to 0^+ \end{cases}\end{aligned} \tag{5.9}$$

for the flat Poincaré sections of de Sitter space. The lower limit of integration has been set so that $\Theta_\gamma = 0$ at $z = \kappa\gamma$, with the corresponding $u_{k\gamma}$ the time at which the Stokes line crosses the real axis: *cf.* (5.19) below. Thus we define κ as the solution of the transcendental equation

$$\sqrt{\kappa^2+1} = \ln\left[\frac{\sqrt{\kappa^2+1}+1}{\kappa}\right] \ \Rightarrow\ \kappa \simeq 0.662743\ . \tag{5.10}$$

As in the constant E-field case, the solutions of the mode eq. (5.4) in persistent or 'eternal' de Sitter space are known analytically. The change of variable to z defined in (5.8) converts (5.3) to Bessel's equation with imaginary index $\pm i\gamma$, so that the solutions may be expressed in terms of $J_{\pm i\gamma}(z)$. The particular linear combination in terms of a Hankel function

$$f_{k\gamma(+)}(u) \equiv \frac{1}{2}\sqrt{\frac{\pi}{H}}\, e^{-\frac{\pi\gamma}{2}} e^{\frac{i\pi}{4}} H^{(1)}_{i\gamma}(z) = \sqrt{\frac{\pi}{H}}\,\frac{e^{\frac{\pi\gamma}{2}} e^{\frac{i\pi}{4}}}{e^{2\pi\gamma}-1}\left[e^{\pi\gamma}J_{i\gamma}(z) - J_{-i\gamma}(z)\right] \tag{5.11}$$

which has been normalized according to (2.4), has the asymptotic behavior

$$f_{k\gamma(+)}(u) \to \frac{e^{iz}}{\sqrt{2Hz}} \leftrightarrow \frac{1}{\sqrt{2H\omega_{k\gamma}}}\exp\left\{-i\Theta_\gamma(z)\right\} \qquad \text{as} \qquad z\to\infty \tag{5.12}$$

matching the positive frequency adiabatic mode $\tilde{f}^{(0)}_k$ in this limit. Thus the solution (5.11) defines the $|0,in\rangle$ vacuum state as $u\to-\infty$ according to the $m^2 - i\epsilon$ prescription, in the flat spatial sections of de Sitter space (5.1). The particular solution (5.11) is also that of the Bunch-Davies state which is $O(4,1)$ de Sitter invariant [2].

On the other hand the particular solution to (5.3)

$$f^{(+)}_{k\gamma}(u) \equiv \frac{\Gamma(1+i\gamma)}{\sqrt{2H\gamma}}\, 2^{i\gamma}\, J_{i\gamma}(z) \to \frac{z^{i\gamma}}{\sqrt{2H\gamma}} \leftrightarrow \frac{1}{\sqrt{2H\omega_{k\gamma}}}\exp\left\{-i\Theta_\gamma(z)\right\} \qquad \text{as} \qquad z\to 0 \tag{5.13}$$

is the properly normalized $|0, out\rangle$ adiabatic vacuum positive frequency solution which agrees with the adiabatic form at late times, $u \to +\infty$, in accordance with (5.9). Since $f^{(+)}_{k\gamma}(u)$ differs from $f_{k\gamma(+)}(u)$, the *in* and *out* vacuum states defined by these positive frequency solutions differ according the Feynman definition. Comparison of (5.13) with (5.11) allows us to read off the exact Bogoliubov coefficients of the scattering problem (2.16)

$$A_\gamma = \frac{\sqrt{2\pi\gamma}\; e^{\frac{i\pi}{4}}}{2^{i\gamma}\,\Gamma(1+i\gamma)}\;\frac{e^{\frac{3\pi\gamma}{2}}}{e^{2\pi\gamma}-1} \tag{5.14a}$$

$$B_\gamma = -\frac{\sqrt{2\pi\gamma}\; e^{\frac{i\pi}{4}}}{2^{i\gamma}\,\Gamma(1+i\gamma)}\;\frac{e^{\frac{\pi\gamma}{2}}}{e^{2\pi\gamma}-1} \tag{5.14b}$$

which are independent of k and satisfy $|A_\gamma|^2 - |B_\gamma|^2 = 1$. The square of the latter coefficient

$$|B_\gamma|^2 = \frac{1}{e^{2\pi\gamma}-1} = e^{-2\pi\gamma}\sum_{n=0}^{\infty} e^{-2\pi n\gamma} \neq 0 \tag{5.15}$$

is the average number of particles created in any $\mathbf{k}$ mode at late times in the CTBD $|0, in\rangle$ state as reckoned by the adiabatic $|0, out\rangle$ vacuum. These exact results tell us that the de Sitter invariant CTBD $|0, in\rangle$ state is not the vacuum state at late times, and is unstable to pair creation, with the average number of particles created at late times given by (5.15).

Moreover from (5.9) the particle creation event takes place at $z \sim \gamma$, at which the adiabatic phase (5.9) transitions from its large z (early time) to its small z (late time) behavior. Applying the complex adiabatic phase method, first using the z variable, reveals again just two complex critical points where the frequency function $\omega^2_{k\gamma}$ vanishes, namely at

$$z = \pm i\gamma \tag{5.16}$$

analogous to (3.12) in the E-field case. Evaluating (5.9) at the complex critical point $-i\gamma$ gives

$$\mathrm{Im}\,\Theta_\gamma(-i\gamma) = \frac{\pi\gamma}{2} \tag{5.17}$$

defining the anti-Stokes lines, and

$$\mathrm{Re}\,\Theta_\gamma(z) = \mathrm{Re}\,\Theta_\gamma(-i\gamma) = 0 \tag{5.18}$$

defining the Stokes lines shown the Fig. 8.

We see from (5.9), (5.18) and Fig. 8 that the Stokes line crosses the real z axis at $z = \kappa\gamma$ or

$$u_{k\gamma} = Ht_{\mathrm{event}}(k) = \ln\left(\frac{k}{\kappa\gamma}\right) \tag{5.19}$$

with κ given by (5.10). This time at which the given k mode experiences its creation event, determined by the global analysis of the Stokes line of the complex adiabatic phase integral crossing the real axis, differs slightly from the time when the local adiabatic condition is maximally violated.

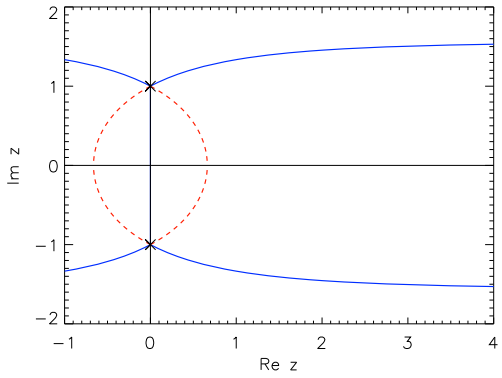

FIG. 8. The solid (blue) lines denote the anti-Stokes lines of constant Im Θ_λ emerging from the two complex turning points of (5.16) with $\gamma = 1$. The dashed (red) lines are the Stokes lines of constant Re Θ_λ connecting the two critical points, the rightmost of which crosses the real axis at $z = \kappa\gamma = \kappa$ given by (5.10).

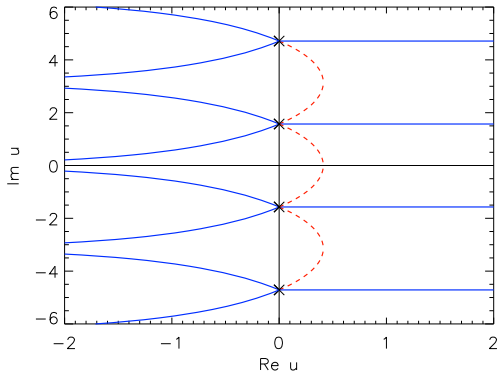

FIG. 9. The Stokes and anti-Stokes lines of Fig. 8 mapped to the complex u plane, for $k = \gamma = 1$, resulting in an infinite number of complex critical points at $u = i\pi\left(n + \frac{1}{2}\right)$ along the imaginary axis, four of which are shown. The solid (blue) lines are the anti-Stokes lines, and the dashed (red) lines are the Stokes lines, one of which crosses the real axis at $u_{k\gamma} = \ln(1/\kappa) = 0.411368$, from (5.19) with $k = \gamma = 1$.

The WKB adiabatic phase also determines the approximate magnitude of particle creation through

$$|B_\gamma|^2 \simeq \exp\left[-4\,\mathrm{Im}\,\Theta_\gamma(-i\gamma)\right] = e^{-2\pi\gamma} \tag{5.20}$$

which agrees with (5.15) calculated from the exact Bessel function solutions of (5.3) only to leading order in $e^{-2\pi\gamma}$ when $\gamma \gg 1$. The reason for this discrepancy (and difference with the exact E-field result) is that the z variable only spans the domain $(0, \infty)$, unlike the infinite range $(-\infty, \infty)$ of the u time variable in the E-field case, so that the complex turning point method utilized previously is not strictly valid in the z variable. On the other hand, if one uses the original $u = Ht$ variable of (5.1), which does run over the infinite time domain, then there are an infinite number of complex turning points, at $u = \ln(k/\gamma) + i\pi\left(n + \frac{1}{2}\right), n \in \mathbb{Z}$, four of which are shown in Fig. 9. The leading order WKB value (5.20) is the contribution from the complex turning point in the upper half u plane nearest to the real axis, which dominates if $\gamma \gg 1$. The infinite series of complex turning

points further the from real axis implies that there are a sum of exponentially smaller contributions in γ from these additional complex turning points, and this is manifest in the exact result (5.15).

The time-dependent adiabatic particle number is defined by eq. (2.15) [5, 43–45, 47] with $f_k = f_{k\gamma(+)}$ of (5.11) for the initial CTBD vacuum, and where to lowest non-vanishing adiabatic order

$$W_k^{(0)} = H\omega_{k\gamma} = H\sqrt{k^2 e^{-2u} + \gamma^2} \tag{5.21a}$$

$$V_k^{(1)} = -\frac{\dot{\omega}_{k\gamma}}{\omega_{k\gamma}} = H\left(1 - \frac{\gamma^2}{\omega_{k\gamma}^2}\right) \tag{5.21b}$$

while to second order in the adiabatic expansion

$$W_k^{(2)} = H\left(\omega_{k\gamma} + \frac{3}{8}\frac{\dot{\omega}_{k\gamma}^2}{\omega_{k\gamma}^3} - \frac{1}{4}\frac{\ddot{\omega}_{k\gamma}}{\omega_{k\gamma}^2}\right) = H\omega_{k\gamma}\,(1+\delta_{k\gamma}) = H\omega_{k\gamma} + \frac{H}{8\,\omega_{k\gamma}}\left(1 - \frac{\gamma^2}{\omega_{k\gamma}^2}\right)\left(1 - \frac{5\gamma^2}{\omega_{k\gamma}^2}\right) \tag{5.22}$$

with $V_k = V_k^{(1)}$ still given by (5.21b). A comparison of $\mathcal{N}_k^{(n)}(u)$ defined by (2.15) for both choices $n = 1, 2$, along with the superadiabatic particle number defined in this case by [51, 52]

$$\overline{\mathcal{N}}_\gamma(u) = \frac{|B_\gamma|^2}{4}\left\{\mathrm{erfc}\left[\frac{-\,\Theta_\gamma(u)}{\sqrt{\mathrm{Im}\,\Theta_\gamma(-i\gamma)}}\right]\right\}^2 = \frac{1}{4\,(e^{2\pi\gamma}-1)}\left\{\mathrm{erfc}\left[-\sqrt{\frac{2}{\pi\gamma}}\,\Theta_\gamma(u)\right]\right\}^2 \tag{5.23}$$

normalized to the correct value of $|B_\gamma|^2$ in (5.15) is shown in Fig. 10. This confirms that the particle number rises rapidly as the Stokes' line is crossed, the global analysis of the adiabatic phase in the complex plane determining most accurately the time of the particle creation event (5.19) [5, 52].

The vacuum decay rate for the expanding half of de Sitter space covered by the Poincaré flat spatial coordinates (5.1) starting in the $|0, in\rangle$ CTBD vacuum can be determined by the Differential Method (2.24). In this case only the magnitude $|\mathbf{k}| = Hk$ is fixed by the Stokes line crossing, so that inverting (5.19)

$$\overline{k}(t) = \kappa\gamma\, e^{Ht} = \kappa\gamma\, a_{\rm dS}(t) \tag{5.24}$$

gives the value of k of the mode experiencing its creation even at time t. Since the integration measure in (2.24) is $d^3\mathbf{k} = H^3\, k^2 dk\, d\Omega_{\hat{\mathbf{k}}}$ and the four-volume factor is $d\mathcal{V}_4 = V a_{\rm dS}^3(t) dt$, we have from (5.24) the Jacobian

$$\left|\frac{d^3\mathbf{k}}{d\mathcal{V}_4}\right|_{k=\overline{k}(t)} = \frac{H^3\, d\Omega_{\hat{\mathbf{k}}}}{V a_{\rm dS}^3}\,\frac{\overline{k}^2 d\overline{k}}{dt} = \frac{\kappa^3\gamma^3 H^4}{V}\, d\Omega_{\hat{\mathbf{k}}} \tag{5.25}$$

which is independent of t, the factors of $a_{\rm dS}^3(t)$ having cancelled. Thus only the integral over the directions of $\hat{\mathbf{k}}$ remains in (2.24), which since $\int d\Omega_{\hat{\mathbf{k}}} = 4\pi$ and $N = 1$ for a single real scalar, gives

$$\Gamma_{\rm dS} = \frac{\kappa^3\gamma^3 H^4}{4\pi^2}\,\ln\left(1 + |B_\gamma|^2\right) = -\frac{\kappa^3\gamma^3 H^4}{4\pi^2}\,\ln\left(1 - e^{-2\pi\gamma}\right) \tag{5.26}$$

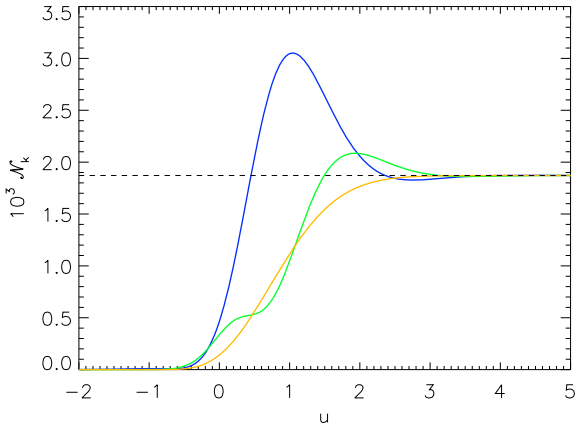

FIG. 10. The mean number of particles created from the vacuum as a function of time in de Sitter space for $\gamma = 1$ and $k = 1$. The three curves are for adiabatic particle numbers $\mathcal{N}_k^{(n)}$ defined by different orders of the asymptotic expansion (2.13) and (5.22)[5], for $n = 1, 2$, and the 'superadiabatic' particle number defined by (5.23) [52]. Note that the zeroth order adiabatic curve (blue) has the highest peak while the superadiabatic curve (orange) has no peak. Although differing somewhat in transient details around $u = u_{k\gamma} = 0.411368$ of (5.19), all three curves rise rapidly from zero near there and tend to the same asymptotic value $|B_\gamma|^2 = 1.87094 \times 10^{-3}$ (dashed line) of (5.15) as $u \to \infty$.

for the decay rate of the CTBD 'vacuum' state of de Sitter space into scalar particle pairs of mass $m = H\sqrt{\gamma^2 + \frac{1}{4}}$, with κ given by (5.10). This result, with the pre-factor determined by the real time Stokes line crossing is a principal result of our analysis. Interestingly $\Gamma_{\rm dS}$ tends to zero in the limit $\gamma \to 0$ as $-\gamma^3 \ln \gamma$, while

$$\Gamma_{\rm dS} \to \frac{\kappa^3 m^3 H}{4\pi^2} \exp\left(-\frac{2\pi m}{H}\right) \qquad \text{for} \quad m \gg H \tag{5.27}$$

in the large mass or flat space limit, similarly to (3.19) for the electric field case. We note from (5.24) that the physical wavelength $(a_{\rm dS}/H\,\overline{k}) = (\kappa\gamma H)^{-1}$ of the Fourier mode at the time of its particle creation event, is of the order of the de Sitter Hubble horizon if $\gamma \sim 1$, but can be much smaller than the horizon if $m \gg H, \gamma \gg 1$.

Note also that although there is no integral over k to perform in (5.26), this value of Γ_{dS} obtained from the Differential Rate definition (2.24) is identical to what would be obtained by an integral rate formula in pure de Sitter space if the de Sitter window step function value of

$$|B_k|^2 = \begin{cases} |B_\gamma|^2\,, & \overline{k}(t_0) \le k \le \overline{k}(t_1) \\ 0\,, & \text{otherwise} \end{cases} \tag{5.28}$$

were used. Because of the kinematic factor of $k^2 dk$ in (2.20) the integral is clearly dominated by the largest value of k contributing at the largest value of the FLRW scale factor for an expanding universe, and one may replace the lower limit of $\overline{k}(t_0) = \kappa\gamma a_{\rm dS}(t_0)$ in (5.28) by zero, in the limit

of large $a_{\rm dS}(t_1) = e^{u_1}$. Thus (2.20) with (5.28) leads again to (5.26), if divided by the integrated four-volume $V \int_{t_0}^{t_1} dt\, a_{dS}^3(t) \to \frac{1}{3H} V e^{3u_1}$ in the same limit.

The result (5.26) is half of what would be obtained in global de Sitter space in leading exponential order for the closed $\mathbb{S}^3$ spatial sections in the same limit, the reason being there are two creation events in each k mode in the closed spatial sections, one in the contracting phase and one in the expanding phase. Thus except for one creation event in each mode as opposed to two, the same phenomenon of vacuum decay takes place in the Poincaré patch of a de Sitter universe that is only expanding, usually considered in FLRW cosmological models, as in the globally complete closed $\mathbb{S}^3$ spatial sections. The vacuum decay rate (5.26) also differs from the result of [3, 5] by a finite pre-factor because of the difference of $N = 1$ *vs.* $N = 2$, and the differing estimate of the constant pre-factor in the K cutoff of the mode sum in (2.20), which is determined to be $\overline{k}(t_1)$ in the present work by the detailed analysis of the particle creation event in real time by the Stokes line crossing.

VI. ADIABATIC SWITCHING DE SITTER ON AND OFF

As in the E-field case, we investigate two different time profiles for switching the de Sitter background on and off, the first with a single adiabatic parameter

$$h(t) \equiv \frac{\dot{a}}{a} = H \,\mathrm{sech}^2(t/T) \tag{6.1}$$

suggested by analogy to (4.1), and the second

$$h(t) \equiv \frac{\dot{a}}{a} = \frac{H}{2} \tanh\left[b\,(t-t_0)\right] - \frac{H}{2} \tanh\left[b\,(t-t_1)\right] \tag{6.2}$$

suggested by the (b, T) E-field profile (4.7) illustrated in Fig. 4.

In the first case (6.1) the FLRW scale factor may be taken to be

$$a(t|T) = \exp\left[HT \tanh(t/T)\right] \tag{6.3}$$

with an arbitrary multiplicative constant of integration set equal to unity. As $t \to \mp\infty$, $a(t|T)$ goes to a constant and the flat space vacua are uniquely defined. Since the solution of the mode eq. (2.2) with (5.2) is not known analytically for this scale factor, we present the numerical results for particle creation $|B_k|^2$ in Fig. 11, which may be compared to Fig. 3. As in the electric field profile (4.1), $|B_k(T)|^2$ falls off at large momenta for any finite T, the falloff becoming more and more gradual as T becomes larger, in which limit a flat plateau at small k characteristic of the constant $h \to H$ de Sitter value (5.15) is attained. Again the $k \to \infty$ (fixed T) and $T \to \infty$ (fixed k) limits of $|B_k(T)|^2$ do not commute, and the gradual falloff of $|B_k(T)|^2$ for those k going through

their creation events when $h(t)$ is not constant makes the FLRW time profile (6.3) inappropriate for the Integral Method of determining the decay rate for pure de Sitter space. However, again as in the case of the one parameter time profile (4.1), the Differential Method for determining the vacuum decay rate of de Sitter space may be applied to the FLRW time profile (6.3) and its $|B_k(T)|^2$ in the adiabatic limit $T \to \infty$, provided the differential Jacobian (5.25) is computed for the modes in the central plateau of Fig. 3 where $h(t) \to H$ is constant. Then the result for pure de Sitter space (5.26) is reobtained.

In the second case of the time profile (6.2), the FLRW scale factor may be taken to be

$$a(t|t_0, t_1, b) = \exp\left\{\frac{H}{2b}\,\ln\left[\frac{\cosh\left[b\,(t-t_0)\right]}{\cosh\left[b\,(t-t_1)\right]}\right] + \frac{H(t_0+t_1)}{2}\right\} \tag{6.4}$$

in which the multiplicative constant of integration has been chosen so that the scale factor has the simple behaviors

$$a(t|t_0, t_1, b) \to \begin{cases} e^{Ht_0} & t \ll t_0 \\ e^{Ht} & t_0 \ll t \ll t_1 \\ e^{Ht_1} & t_1 \ll t \end{cases} \tag{6.5}$$

in each region for $b(t_1 - t_0) \gg 1$. Thus, as in (6.3), the scale factor is a constant in both the very early and very late time limits, the spacetime becomes flat in those limits and again both the $|0, in\rangle$ and $|0, out\rangle$ vacuum states and the particle number are unambiguously well-defined for $t \to \mp\infty$. The k integral in the probability overlap (2.20) again is finite. The de Sitter-like region for $t_0 < t < t_1$ in between can be made arbitrarily long, while the adiabatic turning on and off of the de Sitter background takes a finite time of order b^{-1}, which needs to be large enough so that

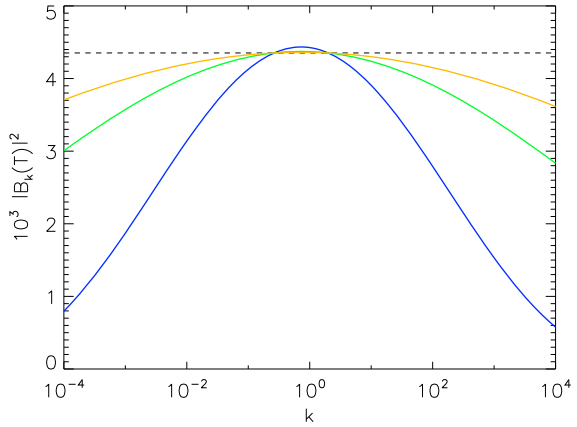

FIG. 11. Particle creation number density $|B_k(T)|^2$ for the one parameter quasi-de Sitter profile (6.1), as a function of k for $m = H$. The curve that falls off the most rapidly in k (blue) is for $HT = 20$, the middle one (green) is for $HT = 40$, and the outer one (orange) is for $HT = 60$, showing the approach to $|B_\gamma|^2 = 4.35228 \times 10^{-3}$ (dashed line) of Eq. (5.15) for small k/a. Compare to Fig. 3.

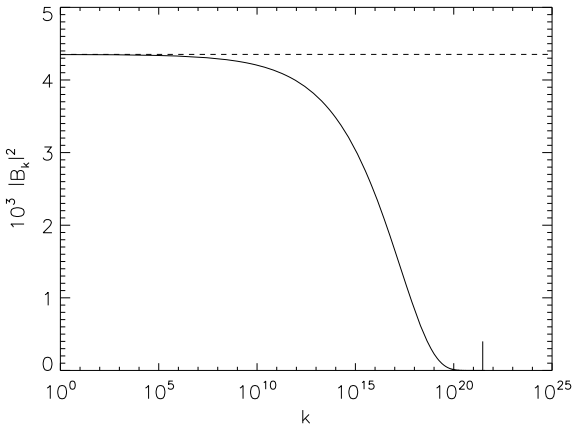

FIG. 12. The mean number density of created particles $|B_k|^2$ in the final state after the de Sitter background is switched off according to the time profile (6.4), for $u_1 \equiv Ht_1 = 50, t_0 = -t_1, b = 0.1\,H$ and $m = H$. The dashed line is the constant (5.15), here 4.35228×10^{-3} expected for pure de Sitter space and $\gamma = \sqrt{3}/2$, and the solid hash marker is the value of $\overline{k} = \kappa\gamma e^{u_1} = 2.97577 \times 10^{21}$ expected from (5.24).

the transition is gentle and adiabatic, and does not in itself lead to significant particle creation. This condition requires that $b \ll H$.

Fig. 12 shows numerical results for the particle number $|B_k|^2$ in the final static region, as $u \to +\infty$. Note that the pure de Sitter value of $|B_k|^2$, (5.15) is obtained for small $k \ll \gamma e^{u_1} \equiv \gamma e^{Ht_1}$. However the falloff from this constant de Sitter 'plateau' value is very gradual unlike the integrand in Fig. 5. The value of $|B_k|^2$ also begins to fall off markedly at k values much smaller than the value $\kappa\gamma e^{u_1}$ expected from (5.24) and (5.15). In the Integral Rate formula (2.23), the integral over dk is weighted by k^2. This integrand is shown in Fig. 13, which because of the falloff of $|B_k|^2$ at large k achieves a maximum value still considerably less than would be expected from the pure de Sitter result (5.15), and at a considerably lower value of k than $\kappa\gamma e^{u_1}$.

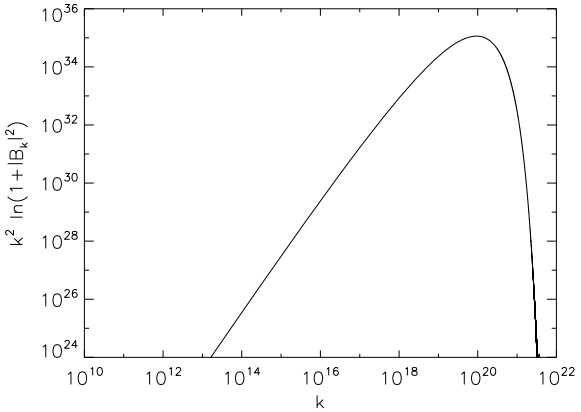

FIG. 13. The decay rate integrand $k^2 \ln(1 + |B_k|^2)$ of (2.23) for the scale factor (6.4) on a log-log plot for the case $u_1 = 50, b = 0.1\,H$ and $m = H$.

In the Integral Method the u_1 volume dependence in the integrated four-volume

$$\mathcal{V}_4 = V \int_{t_0}^{t_1} dt\, a^3(t|t_0,t_1,b) \;\stackrel{u_1\to\infty}{\to}\; \frac{V}{H}\, e^{3u_1}\, F\left(\frac{H}{b}\right) \;\stackrel{b\to 0}{\to}\; \frac{2V}{3H}\, e^{3u_1}\, e^{-\frac{3H}{2b}\ln 2} \tag{6.6}$$

should be cancelled by the range of k integration in the integral $\int k^2 dk \ln(1+|B_k|^2)$ for large $u_1 = Ht_1$. In (6.6) F is a function of H/b which has the small b behavior shown in the second limit. Fig. 14 shows the independence of the value of the plateau level of $|B_k|^2$ for small argument $ke^{-u_1} \to 0$, hence large u_1. This shows that the plateau value of $|B_k|^2$ exists for small enough ke^{-u_1}, and hence from (6.6), the e^{3u_1} scaling expected and needed for the dependence on the final time u_1 to drop out of the rate does indeed hold.

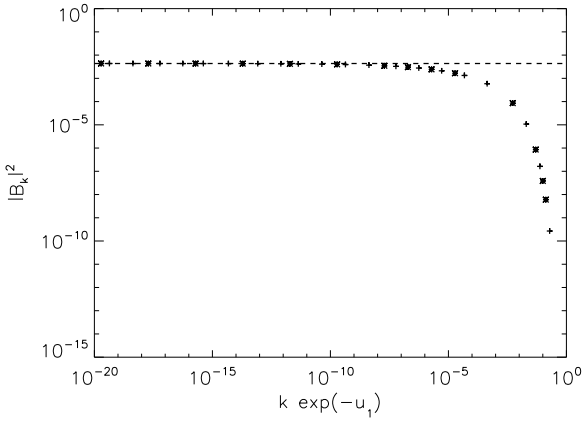

FIG. 14. The mean particle number $|B_k|^2$ as function of rescaled ke^{-u_1} for $u_1 = 50$ (stars) and $u_1 = 70$ (crosses) in the case $b = 0.1\,H, m = H$, showing its universal scaling behavior at large u_1, and de Sitter plateau for $ke^{-u_1} \ll 1$, in agreement with (5.15), expected for pure de Sitter space with $\gamma = \sqrt{3}/2$ (dashed line).

However, if we try to apply the Integral Method (2.23) to define the vacuum decay rate by means of the profile (6.4), the long gradual tail in $|B_k|^2$ as a function of k for larger k, yields a rate that depends on b *no matter how large* u_1 is. In Fig. 15 we show the dependence of $|B_k|^2$ as a function of rescaled ke^{-u_1} for various values of b, showing that the falloff from its de Sitter plateau value depends on b, and occurs at a smaller value of ke^{-u_1} for smaller values of b. This implies a smaller contribution to the integral $\int k^2 dk \ln(1+|B_k|^2)$ for smaller b.

Indeed Fig. 16 shows the numerical results for the decay rate (2.23) turning de Sitter space on and off according to the profile (6.4). As expected, the decay rate rises for large b due to breakdown of the adiabatic condition (2.14) and the creation of particles during the switching on and off of de Sitter space in the short time b^{-1}, coming to dominate over the particle creation in the de Sitter background itself, so we should exclude these large values of b. As b is decreased the rate decreases due to the more rapid falloff of the integrand shown in Fig. 15, reaching a minimum value of (2.23)

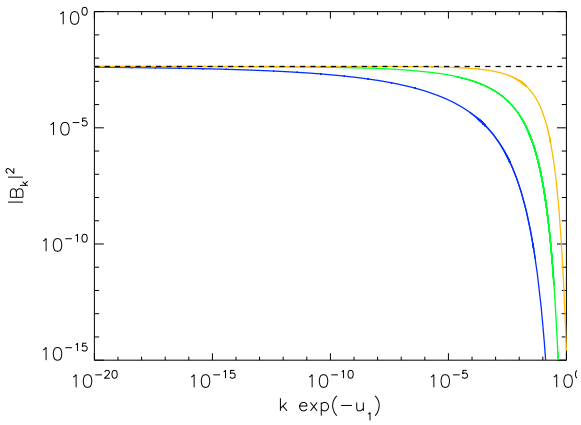

FIG. 15. Mean particle number $|B_k|^2$ *vs.* rescaled momentum ke^{-u_1} for the profile (6.4) for the cases lower to upper of $b = 0.05\,H$ (blue), $b = 0.1\,H$ (green), and $b = 0.2\,H$ (orange). The dashed line is the pure de Sitter value (5.15). For the range of values shown the data for the curves was computed for values of u_1 that are in the scaling range where to a good approximation the value of $|B_k|^2$ depends only on the product ke^{-u_1}. However, the falloff of the tail still depends on b.

at $b \simeq 0.1\,H$, with a rise again for smaller b. This rise for smaller b is the result of the *multiplicative* exponential dependence of $\mathcal{V}_4$ upon b for small $b \ll H$ in the last limit of (6.6), rather than additive dependence in the E-field case.

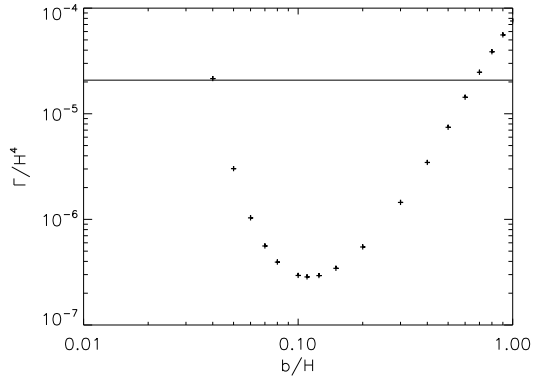

FIG. 16. Numerical results for the decay rate calculated by the Integral Method (2.23) for the scale factor profile (6.4) and integrated four-volume (6.6) as a function of b are shown on a log-log plot for $m = H, \gamma = \sqrt{3}/2$. The horizontal line is the predicted pure de Sitter rate (5.26) of 2.079895×10^{-5} for this value of γ.

The minimum in b shows that there is de Sitter vacuum decay, no matter how slowly or rapidly the de Sitter phase is ended, but that the probability of decay in the profile (6.4) depends upon the time and manner spent exiting the de Sitter phase around $t \sim t_1$, since the b dependence never drops out. This makes the profile (6.4) finally inappropriate for attempting to determine the pure de Sitter vacuum decay rate by the Integral Method (2.23), since the edge effects cannot be eliminated, no matter how large u_1. Indeed the form of $|B_k|^2$ for large k in Figs. 12-14 with its

gradual fall-off from the de Sitter plateau value for the FLRW profile (6.4)-(6.5) actually is more similar to that obtained in the *single parameter* profiles (4.1) or (6.3), in which the deviation from the constant plateau value characteristic of the persistent E-field or de Sitter background cannot be eliminated no matter how large T or u_1 is made.

The failure of the FLRW trial profile (6.4) to reproduce the de Sitter rate (5.26) by the Integral Rate formula (2.23) for arbitrarily large u_1 is nevertheless interesting, and stands in marked contrast to the corresponding calculation with the E-field profile (4.7)-(4.8) in flat space, where the Schwinger rate is recovered in the extrapolation to the limit of of large T in Fig. 6. It shows that there is greater sensitivity to the switching off of the de Sitter background simultaneously over an exponentially large volume at late times in the expansion, arising from both in the dependence upon b of the tail of the particle distribution going through their creation events as the de Sitter phase ends shown in Fig. 15 and the multiplicative exponential dependence on b of the four-volume $\mathcal{V}_4$ in (6.6). Perhaps this greater sensitivity than anything encountered in flat spacetime to how the de Sitter phase is ended over all space uniformly at distances much greater than the de Sitter future event horizon should not be surprising. It suggests that not only is the Bunch-Davies vacuum unstable to particle creation and de Sitter invariance is necessarily broken, no matter how long the de Sitter phase lasts, but that it may be necessary to restrict any spatiotemporal variation of H to within a single causal Hubble horizon, and study the breaking of spatial homogeneity on the horizon scale H^{-1}, as well as time reversal symmetry in de Sitter space.

VII. ENERGY AND PRESSURE OF CREATED PARTICLES: BACKREACTION

The results of the previous sections indicate that so long as the exit from the de Sitter phase is gentle enough, any particles created during that phase end up as particles in the asymptotically static region where the definition of a particle is unambiguous. This shows that the adiabatic particle definition of $\mathcal{N}_k^{(n)}$ for either $n = 1, 2$ used in (5.21) or (5.22) during the de Sitter phase [5] is robust and survives in the final asymptotic flat space region as $|B_{\mathbf{k}}|^2$. There is no doubt that these are the real particles observed in the final state after the time-dependent background has been turned off. This may be verified also by evaluating the energy density and pressure of the created particles. After subtracting the vacuum value of the stress tensor components obtained by setting $A_{\mathbf{k}} = 1, B_{\mathbf{k}} = 0$, we obtain for the renormalized flat space energy density simply [44, 45]

$$\rho = \langle T_{tt} \rangle_R = \frac{1}{a^3} \int \frac{d^3\mathbf{k}}{(2\pi)^3} \, \omega_{\mathbf{k}} \, |B_{\mathbf{k}}|^2 \tag{7.1}$$

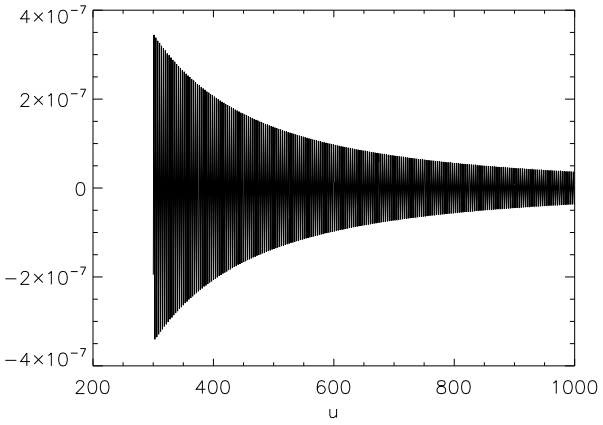

FIG. 17. The phase coherent oscillating part of the pressure, given by the last term in (7.2), for $\xi = \frac{1}{6}, m = H, u_1 = 10$, and $b = H$. The envelope of the rapid oscillations falls as $1/u^2$ at late times.

where $\omega_{\mathbf{k}}$ and $a \to e^{u_1}$ are the constant values of the frequency (5.2) and scale factor in the asymptotic late time for the profile (6.4)-(6.5) after the expansion has been turned off and spacetime is again flat. The corresponding expression for the renormalized isotropic pressure is

$$p = \frac{1}{3a^3}\int \frac{d^3\mathbf{k}}{(2\pi)^3}\left(\omega_{\mathbf{k}} - \frac{m^2}{\omega_{\mathbf{k}}}\right)|B_{\mathbf{k}}|^2 + \frac{1}{3a^3}\int \frac{d^3\mathbf{k}}{(2\pi)^3}\left[2\,(6\xi-1)\,\omega_{\mathbf{k}} - \frac{m^2}{\omega_{\mathbf{k}}}\right]\mathrm{Re}\left(A_{\mathbf{k}}B^*_{\mathbf{k}}e^{-2i\omega_{\mathbf{k}}t}\right) \quad (7.2)$$

in flat space, where $6\xi - 1 = 0$ in the present study. Note that because of the scaling behavior of $|B_k|^2$ illustrated in Fig. 14, the change of variable from $\mathbf{k}$ to $\mathbf{k}/a$ shows that both the energy density and the pressure are *constants, independent* of the length of time u_1 spent in the de Sitter phase. In other words ρ and p *do not redshift to zero* with the exponential de Sitter expansion. The reason for this is that although each k mode certainly does redshift with the expansion, particles are continually being created at the latest time u_1 to replenish them at the largest $k \sim \overline{k}(t_1) = \kappa\gamma e^{u_1}$, so that the integrals (7.1) and (7.2) are independent of u_1.

If these integrals are evaluated for the pure de Sitter window value (5.28) and large u_1, then making the change of variable (5.8) we obtain

$$\begin{aligned}\rho &= \frac{H^4\,|B_\gamma|^2}{2\,\pi^2}\int_0^{\kappa\gamma} dz\, z^2\left(z^2+\frac{m^2}{H^2}\right)^{\frac{1}{2}} \\ &= \frac{H^4\,|B_\gamma|^2}{16\,\pi^2}\left\{z\left(2z^2+\frac{m^2}{H^2}\right)\left(z^2+\frac{m^2}{H^2}\right)^{\frac{1}{2}} - \frac{m^4}{H^4}\ln\left(\frac{H}{m}\left[z+\left(z^2+\frac{m^2}{H^2}\right)^{\frac{1}{2}}\right]\right)\right\}_{z=\kappa\gamma} \quad (7.3a)\end{aligned}$$

$$\begin{aligned}p &= \frac{H^4\,|B_\gamma|^2}{6\,\pi^2}\int_0^{\kappa\gamma} dz\, z^4\left(z^2+\frac{m^2}{H^2}\right)^{-\frac{1}{2}} \\ &= \frac{H^4\,|B_\gamma|^2}{16\,\pi^2}\left\{z\left(\frac{2}{3}z^2-\frac{m^2}{H^2}\right)\left(z^2+\frac{m^2}{H^2}\right)^{\frac{1}{2}} + \frac{m^4}{H^4}\ln\left(\frac{H}{m}\left[z+\left(z^2+\frac{m^2}{H^2}\right)^{\frac{1}{2}}\right]\right)\right\}_{z=\kappa\gamma} \quad (7.3b)\end{aligned}$$

where $|B_\gamma|^2$ is given by (5.15), κ is given by (5.10), we have taken $\xi = \frac{1}{6}$ and also neglected the last interference term in (7.2). This is justified because as shown in Fig. 17, this term oscillates rapidly

in the static out region and vanishes in the late time limit, just as the oscillating $A_{\mathbf{k}}B^*_{\mathbf{k}}$ quantum interference term in the electric current does at late times illustrated in the Left Panel of Fig. 7.

Because of the rapid oscillations and their damping in evidence in Fig. 17, there is very effective phase decoherence or *dephasing* in these terms, and the contribution of the interference term in the mean pressure washes out. This behavior is related to the fact that $|B_{\mathbf{k}}|^2$ and the diagonal elements of the density matrix in the particle basis (2.18) or (2.21) are *adiabatic invariants*, whereas the $A_kB^*_k$ interference terms and off-diagonal elements of the density matrix depend upon the phase $\exp(-2i\Theta_{\mathbf{k}})$, which oscillates rapidly as a function of either t or k in flat space. Thus, the rapidly oscillating off-diagonal element of the density matrix in the final state basis may be neglected, and the initial pure vacuum state $|0, in\rangle$ may be treated as a mixed state with positive entropy in the late time *out* basis. In this approximation, well-justified by the behavior of the pressure term illustrated in Fig. 17, the particle creation, in principle unitary and reversible if all exact phase correlations are preserved, becomes effectively Markovian and irreversible [47].

The values of the energy and pressure in the asymptotic final state are independent of the duration of the de Sitter phase because of the scaling illustrated in Fig. 14, and both are *positive*, as might have been expected for real particles. Thus the stress tensor of the created particles is completely unlike that in the 'eternal' expanding de Sitter background, where the stress tensor tends to the de Sitter invariant Bunch-Davies attractor value with $\rho + p = 0$, all initial state deviations from this value falling exponentially with time [8]. This occurs because the oscillatory phase coherent terms do *not* wash out at late times in fixed de Sitter space, as they do in Fig. 17, but instead give a contribution of the same order as that of the created particles, combining with them to give the de Sitter invariant value at late times. This phase coherence is due to the fact that all the Fourier modes in the broad range of values $\gamma \ll k \lesssim \gamma a(t)$ remain in phase, because of the exponential suppression of both the t and k dependence of (5.9), through $k/a = ke^{-Ht}$ in de Sitter space. Thus as these modes pass outside the de Sitter Hubble horizon, they have nearly the same time dependence and add coherently in the integral over k, remaining of the same order as the particle creation terms. Our results show that this phase coherence of superhorizon modes in pure de Sitter space is destroyed by the transition out of de Sitter, however gentle, while the particle number term $|B_k|^2$ is robust, surviving the transition due to its adiabatic invariance.

In order to estimate the backreaction of the created particles, we note that the Einstein equation

$$\frac{dH}{dt} = -4\pi G\,(\rho + p) < 0 \tag{7.4}$$

for $\rho+p > 0$ in the final state, tends to decrease the curvature, assuming that the phase coherence of

the superhorizon modes is not preserved and the particle contributions dominate the stress tensor. From Eqs. (7.3) we have

$$\rho + p = \frac{H^4 \, |B_\gamma|^2 \gamma^3}{6\pi^2} \, \kappa^3 \left(\kappa^2 \gamma^2 + \frac{m^2}{H^2} \right)^{\frac{1}{2}} > 0 \tag{7.5}$$

so that (7.4) leads to a fractional decrease in the expansion rate of order

$$\frac{\Delta H}{H} \simeq -\frac{2}{3\pi} \, G H^2 \, \frac{\gamma^4 \, \kappa^3}{e^{2\pi\gamma} - 1} \left(\kappa^2 + 1 + \frac{1}{4\gamma^2} \right)^{\frac{1}{2}} \tag{7.6}$$

for a Hubble expansion time $H\Delta t \simeq 1$. The backreaction is small if $GH^2 \ll 1$ and contains the additional exponential suppression from $|B_\gamma|^2$ as in (5.27) if $m \gg H$. It is nevertheless non-zero and appears at one-loop order even for a massive free field, in contrast to quantized graviton contributions reported at two-loop order in [20].

Note that although the energy density and pressure (7.3) are not exponentially redshifted away due to the constant rate of particle creation in de Sitter space, neither do they grow in the time T that the de Sitter phase persists, as the electric current does in the E-field case, *c.f.* Fig. 7. In the E-field case the created particles are accelerated to relativistic velocities after their creation and contribute a current which grows linearly with the window of modes that go through their creation events, and hence that grows secularly with time, producing a backreaction effect on the electric field that clearly must eventually be taken into account in a consistent dynamical system. This acceleration of created particles to relativistic velocities appears more similar to the contracting part of the time slicing of the full de Sitter hyperboloid, in which the created particles are blueshifted rather than redshifted and exponentially growing stress-energy perturbations occur [5, 6].

VIII. DISCUSSION

In this paper we have presented a detailed analysis of particle creation and vacuum decay in persistent background fields that are homogeneous in space, such as the constant uniform electric field and de Sitter space. The vacuum state of QFT in the presence of such background external fields is specified not by analytic continuation to Euclidean time, but by the Feynman-Schwinger $m^2 - i\epsilon$ causal prescription which defines particle and antiparticle excitations in *real* time. This defines a scattering problem (2.16) for massive scalar fields which determines the mean particle number created in pairs in each Fourier mode, and relates the vacuum persistence probability (2.20) directly to the number of created particles. The zero overlap between the $|0, in\rangle$ and $|0, out\rangle$ states

in (1.1) in the strict limit of infinite four-volume is no pathology, but simply a consequence of a constant vacuum decay rate Γ per unit time per unit volume in a persistent background field. The four-volume $\mathcal{V}_4$ factor must be removed in order to obtain a well-defined vacuum decay rate.

By analyzing the particle creation process in real time, we have given an invariant Differential Rate formula (2.24) for the vacuum decay rate in such persistent fields in which no divergent integrals over momenta are encountered. The evaluation of this Differential Rate relies upon an analysis of the critical points of the adiabatic phase integral (2.9) in the complex time domain, and the semi-classical definition of the time at which this particle creation can be said to occur. This time $t_{\rm event}(\mathbf{k})$ is defined by the point at which the Stokes line of constant Real Part of the adiabatic phase for the given Fourier mode $\mathbf{k}$ crosses the real time axis, and thereby gives a relation between $\mathbf{k}$ and t that determines the Jacobian in (2.24). In the case of the constant, uniform electric field, Schwinger's result for the decay of the vacuum into charged particle/antiparticle pairs is recovered in this way. In the case of de Sitter space, the pre-factor of the Bunch-Davies vacuum decay rate, somewhat ill-defined in earlier treatments, is also fixed, with the principal result being (5.26).

We have also discussed an Integral Method (2.23) for calculating the vacuum decay rate in persistent background fields. This method relies upon replacing the external field extending infinitely to the past and future in time, by one which is adiabatically switched on from zero around some finite time t_0, allowed to persist for a long but finite time until t_1, and then adiabatically switched off again. This defines the total number of particles in the asymptotic final state unambiguously, and verifies that the adiabatic particle number definition (2.15) $\mathcal{N}_k^{(n)}$ for either $n = 1, 2$ is robust, giving the correct average number of asymptotic particles in a given Fourier mode after the background electric or gravitational field is turned off. For this Integral Method of defining the vacuum decay rate of a persistent field to work, it is necessary to find a time dependent background for which any effects associated with switching the background field on and off can be made negligibly small in the limit $T = t_1 - t_0 \to \infty$. We found a suitable two-parameter family of external gauge potentials (4.7) for which this condition is satisfied, and once again found the same Schwinger decay rate for a long-persistent uniform electric field by this Integral Method.

In the case of de Sitter space, the apparently natural generalization of this two-parameter FLRW background spacetime (6.4) does *not* yield the de Sitter decay rate, because the asymptotic particle number at large k depends upon the time scale b^{-1} with which the de Sitter background is turned off at late times, no matter how long the de Sitter phase lasts. Since the two-parameter FLRW background (6.4) requires the switching off of de Sitter background curvature everywhere in space in cosmic time, far outside the de Sitter-Hubble horizon, one might suspect that this spatially

homogeneous background is particularly artificial, and perhaps should be replaced with one that is regulated also in its spatial extent at the horizon scale. The failure of the Integral Method for strictly spatial homogeneous switching on/off of de Sitter space is indicative of a greater sensitivity of de Sitter space to the long wavelength modes lying outside their causal Hubble horizon, and hence to spatial boundary conditions.

The main conclusion to be drawn from the existence of particle creation and a non-zero decay rate (5.26) starting from the de Sitter invariant Bunch-Davies state is that this CTBD state is not a stable ground state of QFT in de Sitter space, and that $SO(4,1)$ de Sitter symmetry is necessarily broken, both in time, and possibly also in space, even by a free massive quantum field without self-interactions. Stated differently, the Feynman-Schwinger $m^2-i\epsilon$ definition of the vacuum of QFT and particle excitations is incompatible with the requirements of de Sitter invariance, at least for conformally coupled massive scalar fields with any finite $m > H/2$, for which the particle concept is well-defined. In de Sitter space, analogously to the constant electric field background, for which a time independent Hamiltonian bounded from below also does not exist, the $m^2-i\epsilon$ definition of particle excitations implies spontaneous vacuum decay and the spontaneous breaking of the time reversal symmetry of the background [56].

Since the Feynman-Schwinger $m^2-i\epsilon$ condition goes smoothly over to that of the standard Minkowski vacuum for any slowly time-varying adiabatic background, whether electromagnetic or gravitational, independent of any symmetry of the background, analyticity in the mass parameter is a more general principle of determination of the vacuum of QFT, more firmly based on physical considerations of causality than the Euclidean postulate. The compatibility of Wick rotation in time to the $m^2-i\epsilon$ prescription is a special property of zero-field Minkowski space where Poincaré invariance dictates that correlation functions at x and x' can only be a function of $m^2(x-x')^2 = -m^2(t-t')^2 + m^2(\mathbf{x}-\mathbf{x}')^2$, with the result that analyticity in m^2 and Euclidean continuation are necessarily related. This equivalence cannot be assumed in general, and in particular it ceases to hold when additional parameters of the background field enter the time dependence of correlation functions, when there is no invariant decomposition into positive and negative frequency subspaces, or when a Hamiltonian bounded from below does not exist in real time, as in de Sitter space, in which cases continuation to Euclidean time has no evident physical justification.

On any given FLRW time slice of constant t in the spatially flat coordinates (5.1), the physical adiabatic vacuum is Bunch-Davies only for Fourier modes with wave numbers $k \gg \overline{k}(t) = \kappa\gamma e^{Ht}$, while for modes with $k \ll \overline{k}(t)$ the vacuum state is described by the positive frequency *out* mode functions (5.13), with a smooth but fairly rapid switchover at $k \sim \overline{k}(t)$, illustrated in Fig. 10. Since

modes continue to redshift with the de Sitter expansion, the dividing line $\overline{k}(t)$ between the modes in the Bunch-Davies vacuum and those whose vacuum state is defined by (5.13) continues to grow in co-moving wavenumber k. This implies that particles are continuously created at $k \sim \overline{k}(t)$, and both the vacuum decay rate and the total energy density and pressure (7.3) of the created particles are *independent* of the duration of the de Sitter expansion.

These particles surviving after the de Sitter background has been switched off contribute a constant positive energy density and pressure in the final state, which does not redshift away, no matter how long the de Sitter phase persists. Since $\rho + p > 0$, this suggests that the stress-energy of the created particles will create a backreaction that will decrease the effective cosmological 'constant' over time. We have estimated the magnitude of the backreaction effect by (7.4)-(7.6) in the case that exact spatial homogeneity is preserved, assuming the quantum phase oscillation $A_{\mathbf{k}}B^*_{\mathbf{k}}$ interference terms can be neglected. This estimate of the backreaction (7.6) is small for massive fields if $GH^2 \ll 1$. Nevertheless *any* instability of de Sitter space due to particle creation effects indicates that the Bunch-Davies state is not the stable ground state of QFT coupled to Einstein gravity with a cosmological constant, and that quantum particle creation effects should be taken into account in a fully consistent backreaction calculation. We have not considered light or massless fields in this paper, but one may suspect that their backreaction effects could be significantly larger.

In contrast to these results stands the fact that in fixed eternal de Sitter space the $O(4,1)$ de Sitter invariant Bunch-Davies state for a conformally coupled massive scalar field possesses a renormalized mean field stress-energy tensor $\langle T_{\mu\nu}\rangle$ proportional to $g_{\mu\nu}$. Hence it induces only a constant vacuum energy with $p = -\rho$, that can be absorbed into a finite renormalization of the cosmological constant, resulting in a self-consistent semi-classical solution with full de Sitter symmetry [57]. Since the propagator in the Bunch-Davies state possesses the short distance Hadamard behavior matching to that of flat space, making it normalizable and UV allowed, and since it is the only de Sitter invariant state with this property [3, 45], it is often considered a preferred 'vacuum' state, apart from any appeal to continuation to Euclidean time. Despite the particle creation, if all terms in the renormalized $\langle T_{\mu\nu}\rangle$ are taken into account in a *fixed* de Sitter background, the stress-energy remains de Sitter invariant and fixed at its Bunch-Davies value. Moreover in this fixed expanding de Sitter background the expansion even drives initial state perturbations in $\langle T_{\mu\nu}\rangle$ back to its Bunch-Davies value at late times [8]. Thus the late time pure de Sitter limit is quite different and *not* equal to the late time limit of a FLRW time profile such as (6.4), no matter how large the finite time t_1 is taken, and no matter how gently the de Sitter phase ends.

These facts are in no way inconsistent with each other, since the interference terms of the

superhorizon modes act to cancel the particle creation terms in the CTBD state in exact de Sitter space, but go to zero if the de Sitter background is switched off, as Fig. 17 shows. The mere existence of a de Sitter invariant state, however 'natural' it might appear to be, is also not sufficient to insure its stability. The adiabatic vacuum, agreeing with the Bunch-Davies state for large $k \gg \overline{k}(t) = \kappa\gamma e^{Ht}$ is also UV allowed, and physically preferred according to the Feynman-Schwinger $m^2 - i\epsilon$ definition. We have shown in this paper that by this definition, the completely de Sitter symmetric Bunch-Davies state is *not* the vacuum state of de Sitter space at late times, but instead contains a definite mean number of particle excitations above the physical $|0, out\rangle$ vacuum. We emphasize that although the particles are clearly seen to be real in the flat spacetime region after the de Sitter background is turned off according to the profile (6.4), the particles in the plateau for $k \ll e^{u_1}$ in Figs. 14-15 are created in de Sitter space itself, not in the transition out of de Sitter space, and the Differential Decay Rate (5.26) is explicitly due to this de Sitter particle creation, and not to any effect of the transition.

Nevertheless the cancellation of the particle creation terms and reversion to the Bunch-Davies value in de Sitter space does present us with the question of what actually happens in a fully self-consistent evolution, rather than one in which the de Sitter background is either artificially eternally fixed or artificially turned off. What are the implications of the particle creation and decay rate (5.26) of the initial Bunch-Davies 'vacuum' state in the true physical situation of fully dynamical gravitational plus matter fields?

At this point we can attempt an answer to this important question only in the form of a speculation based on known infrared effects in gravitational systems and analogies with better studied many-body systems. The semi-classical Einstein eqs. with source $\langle T_{\mu\nu} \rangle$ amount to a large N mean field approximation, in which the N matter fields interact with the classical gravitational field, but not directly with each other [47, 54]. The gravitational interaction between the created particles of the matter appears at first order in $1/N$ [58]. Since these created particles are redshifted to very small physical momenta at late times by the expansion, and the gravitational interaction is long range, these $1/N$ interaction terms, completely ignored in the leading order, can lead to contributions to the next order stress-energy tensor which grow secularly in time. This behavior is generic to $1/N$ corrections to mean field evolution in nonequilibrium systems [59], and has been seen both in electric field backgrounds [60], and inflationary models [10, 17, 19, 20, 61].

Thus the behavior of the long wavelength Fourier modes may well be quite different than in the leading order semi-classical mean field description. Although the full solution of infrared problems in dynamical cosmologies, or even full QED, is still lacking, experience with other systems suggest

that sophisticated resummation methods are required to capture the leading order secular terms, leading to decoherence, entropy generation and irreversible behavior [59, 62], for which a coarse grained stress-energy tensor may be appropriate [63]. If interactions are taken into account through Boltzmann transport equations, the adiabatic particle definition also provides the link between QFT and a fully classical (completely phase incoherent) particle limit. Clarifying these issues and the behavior of the long wavelength modes in a fully dynamical cosmology certainly will require the specification of the QFT vacuum both in and out of the de Sitter phase. The full solution could have important consequences for the reheating of the universe at the end of inflation, and predictions for the Cosmic Microwave Background observed today.

Finally the sensitivity of the rate (16) on how the de Sitter phase ends, simultaneously over all space at late times in the time profile (6.4), and the possibility of significant backreaction effects and departure from the mean field evolution on the horizon scale may be related. If the persistent de Sitter background were to be regulated differently, in a way consistent with a finite causal Hubble horizon, by modifying it with a spatial regulator rather than switching it on and off in FLRW time everywhere in space, the superhorizon modes would be treated quite differently, or cut off entirely. Hence it appears likely that sensitivity to spatial boundary conditions through a regulator or other physics on the horizon scale will survive in a more complete treatment. If so, or if infrared interaction effects are significant at this scale, this would imply spatial homogeneity is broken on the horizon scale H^{-1}, leading to a spatially inhomogeneous rather than global FLRW cosmology. Evidence for the additional breaking of spatial homogeneity, as well as time reversal inherent in vacuum decay of de Sitter space, due to the conformal anomaly was presented previously in Ref. [6, 64]. If spatial homogeneity is broken, then the backreaction of the created particles in a spatially inhomogeneous universe should be considered, and vacuum dark energy, rather than being a spacetime constant, will acquire spatial as well time dependence on the scale of the Hubble horizon, with potentially far-reaching consequences for observational cosmology, continuing to the present quasi-de Sitter epoch.

ACKNOWLEDGMENTS

E. M. acknowledges a stimulating discussion with A. M. Polyakov prior to publication of this work, and useful comments on a first draft by E. T. Akhmedov, C. Burgess, and S. A. Fulling. This work was supported in part by the National Science Foundation under Grants No. PHY-0856050, No. PHY-1308325, and No. PHY-1505875 to Wake Forest University and by a Wake Forest

University Bridge Grant. Some of the numerical work was done using the WFU DEAC cluster; we thank the WFU Provost's Office and Information Systems Department for their generous support. Numerical work relating to this project was also done using the OIT henry2 cluster at North Carolina State University.

References

[1] N. A. Chernikov and E. A. Tagirov, *Ann. Inst. H. Poincaré Phys. Theor.* **A9**, 109 (1968); E. A. Tagirov, *Ann. Phys.*, **76**, 561 (1973).

[2] T. S. Bunch and P. C. W. Davies, *Proc. R. Soc. A* **360**, 117 (1978).

[3] E. Mottola, *Phys. Rev. D* **31** 754 (1985).

[4] A. M. Polyakov, *Nucl. Phys. B* **797**, 199 (2008); *ibid.* **834**, 316 (2010); e-print arXiv:1209.4135; D. Krotov and A. M. Polyakov, *Nucl. Phys. B* **849**, 410 (2011).

[5] P. R. Anderson and E. Mottola, *Phys. Rev. D* **89** 104038 (2014).

[6] P. R. Anderson and E. Mottola, *Phys. Rev. D* **89** 104039 (2014).

[7] A. D. Dolgov, M. B. Einhorn, and V. I. Zakharov, *Phys. Rev. D* **52**, 717 (1995).

[8] P. R. Anderson, W. Eaker, S. Habib, C. Molina-París, and E. Mottola, *Phys. Rev. D* **62**, 124019 (2000).

[9] N. P. Myhrvold, *Phys. Rev. D* **28**, 2439 (1983).

[10] E. T. Akhmedov and P. V. Buividovich, *Phys. Rev. D* **78**, 104005 (2008).

[11] A. Higuchi, *Class. Quant. Grav.* **26**, 072001(2009).

[12] J. Bros, H. Epstein, and U, Moschella, *Ann. Inst. H. Poincaré* **11**, 611 (2010).

[13] D. Marolf and I. A. Morrison, *Phys. Rev. D* **82**, 105032 (2010); *ibid.* **84**, 044040 (2011); *Gen. Rel. Grav.* **43**, 3497 (2011).

[14] J. Serreau, *Phys. Rev. Lett.* **107**, 191103 (2011).

[15] D. Boyanovsky and R. Holman, *J. High Ener. Phys.* **2011**, 47 (2011).

[16] D. P. Jatkar, L. Leblond, and A. Rajaraman, *Phys. Rev. D* **85**, 024047 (2012).

[17] E. T. Akhmedov, *J. High Ener. Phys.* **2012**, 066 (2012); *Phys.Rev. D* **87**, 044049 (2013).

[18] S. Hollands, *Comm. Math. Phys.* **319**, 1 (2013).

[19] E. T. Akhmedov, *Int. J. Mod. Phys. D* **23**, 1430001 (2014); E. T. Akhmedov, U. Moschella, K. E. Pavlenko, and F. K. Popov *Phys. Rev. D* **96**, 025002 (2017).

[20] N. C. Tsamis and R. P. Woodard, *Nuc. Phys. B* **474**, 235 (1996); *Ann. Phys.* **253**, 1 (1997); *ibid.* **267**, 145 (1998).

[21] S. Dodelson, *Modern Cosmology*, Elsevier Science, Amsterdam (2003); V. F. Mukhanov, *Physical Foundations of Cosmology*, Cambridge Univ. Press, Cambridge (2005).

[22] S. Weinberg, *Rev. Mod. Phys.* **61**, 1 (1989).

[23] T. Padmanabhan, *Phys. Reports* **380**, 235 (2003).

[24] I. Antoniadis, P. O. Mazur and E. Mottola, *New J. Phys.* **9**, 11 (2007).

[25] J. Schwinger, *Phys. Rev.* **82**, 664 (1951);
See also E. Brezin and C. Itzykson, *Phys. Rev. D* **2**, 1191 (1970).

[26] N. B. Narozhnyi, *Zh. Eksp. Teor. Fiz.* **54**, 676 (1968) [Sov. Phys. JETP **27**, 360 (1968)].

[27] A. I. Nikishov, *Zh. Eksp. Teor. Fiz.* **57**, 1210 (1970) [Sov. Phys. JETP **30**, 660 (1970)].

[28] N. B. Narozhnyi and A. I. Nikishov, *Yad. Fiz.* **11**, 1072 (1970) [Sov. J. Nuc. Phys. **11**, 596 (1970)].

[29] E. S. Fradkin, D. M. Gitman, and Sh. M. Shvartsman, *Quantum Electrodynamics with Unstable Vacuum*, Springer-Verlag, Berlin (1991).

[30] S. O. Gavrilov and D. M. Gitman, *Phys. Rev. D* **53**, 7162 (1996).

[31] R. P. Feynman, *Phys. Rev.*, **76**, 749 (1949); *ibid.* 769 (1949).

[32] E. C. G. Stueckelberg, *Helv. Phys. Acta* **14**, 588 (1941).

[33] B. S. DeWitt, *Dynamical Theory of Groups and Fields*, Gordon and Breach, New York (1965);
Phys. Rep. **19**, 295 (1975).

[34] H. Rumpf, *Phys. Lett. B* **61**, 272 (1976); *Nuovo Cim. B* **35**, 321 (1976);
H. Rumpf and H. K. Urbantke, *Ann. Phys.* **114**, 332 (1978).

[35] H. Rumpf, *Phys. Rev. D* **24**, 275 (1981).

[36] O. Nachtmann, *Commun. Math. Phys.* **6**, 1 (1967).

[37] L. Parker, *Phys. Rev. Lett.* **21**, 562 (1968); *Phys. Rev.* **183**, 1057 (1969); *Phys. Rev. D* **3**, 346 (1971), Erratum *ibid.* 2546 (1971); *Phys. Rev. Lett.* **28**, 705 (172), Erratum *ibid.* 1497 (1972).

[38] Ya.B. Zel'dovich, *Pis. Zh. Eksp. Teor. Fiz.* **12**, 443 (1970) [JETP Lett. **12**, 307 (1970)].

[39] L. Parker and S. A. Fulling, *Phys. Rev. D* **9**, 341 (1974);
S. A. Fulling and L. Parker, *Ann. Phys.* **87**, 176 (1974);
S. A. Fulling, L. Parker, and B. L. Hu, *Phys. Rev. D* **10**, 3905 (1974).

[40] N. D. Birrell and P. C. W. Davies, *Quantum Fields in Curved Space*, Cambridge Univ. Press, Cambridge (1982).

[41] M. Born and V. Fock, *Z. Phys.* **51**, 165 (1928).

[42] N. D. Birrell, *Proc. R. Soc. Lon. B* **361**, 513 (1978);
T. S. Bunch, *J. Phys. A: Math. Gen.* **13**, 1297 (1980).

[43] Y. Kluger, E. Mottola, and J. M. Eisenberg, *Phys. Rev. D* **58**, 125015 (1998).

[44] S. Habib, C. Molina-París, and E. Mottola, *Phys. Rev. D* **61**, 024010 (2000).

[45] P. R. Anderson, C. Molina-París, and E. Mottola, *Phys. Rev. D* **72**, 043515 (2005).

[46] L. S. Brown and S. J. Carson, *Phys. Rev. A* **20**, 2486 (1979).

[47] S. Habib, Y. Kluger, E. Mottola, and J. P. Paz, *Phys. Rev. Lett.* **76**, 4660 (1996);
F. Cooper, S. Habib, Y. Kluger, and E. Mottola, *Phys. Rev. D* **55**, 6471 (1997).

[48] V. L. Pokrovskii and I. M. Khalatnikov, *Zh. Eksp. Teor. Fiz.* **40**, 1713 (1961) [Sov. Phys. JETP **13**, 1207 (1961)].

[49] J. Audretsch, *J. Phys. A: Math. Gen.* **12**, 1189 (1979).

[50] N. Fröman and P. O. Fröman, *Physical Problems Solved by the Phase Integral Method*, Cambridge Univ. Press, Cambridge (2002).

[51] M. V. Berry, *Proc. R. Soc. A* **422**, 7 (1989); *ibid.* **427**, 265 (1990); *J. Phys. A* **15**, 3693 (1982).

[52] R. Dabrowski and G. V. Dunne, *Phys. Rev. D* **90**, 025021 (2014).

[53] F. Sauter, *Z. Phys.* **73**, 547 (1931).

[54] Y. Kluger, J. M. Eisenberg, B. Svetitsky, F. Cooper, and E. Mottola, *Phys. Rev. Lett.* **67**, 2427 (1991); *Phys. Rev. D* **45**, 4659 (1992);
F. Cooper, J. M. Eisenberg, Y. Kluger, E. Mottola, and B. Svetitsky, *Phys. Rev. D* **48**, 190 (1993).

[55] F. Gürsey, *Ann. Phys.*, **24**, 211 (1963);
G. Börner and H. P. Dürr, *N. Cimento*, **64A**, 669 (1969).

[56] E. Mottola, *Phys. Rev. D* **33**, 2136 (1986); *Physical Origins of Time Asymmetry*, J. J. Halliwell *et al.* eds., pp. 504-515, Cambridge, Cambridge Univ. Press (1993).

[57] S. Wada and T. Azuma, *Phys. Lett. B* **132**, 313 (1983).

[58] F. Cooper, S. Habib, Y. Kluger, E. Mottola, J. P. Paz, and P. R. Anderson, *Phys. Rev. D* **50**, 2848 (1994).

[59] J. Berges, *AIP Conf. Proc.* **739**, 3 (2005).

[60] E. T. Akhmedov, N. Astrakhantsev, and F. K. Popov, *J. High Ener. Phys.* **1409**, 071 (2014); *ibid.* **1509**, 085 (2015).

[61] D. Seery, *Class. Quant. Grav.* **27**, 124005 (2010);
C. P. Burgess, R. Holman, and G. Tasinato, *J. High Ener. Phys.* **1601**, 153 (2016).

[62] S. Jeon, *Phys. Rev. D* **52**, 3591 (1995).

[63] T. Markkanen, *J. Cosmol. Astropart. Phys.* **11** (2016) 026; e-print arXiv:1703.06898.

[64] P. R. Anderson, C. Molina-París, and E. Mottola, *Phys. Rev. D* **80**, 084005 (2009).